JOURNAL OF PHYSICAL ORGANIC CHEMISTRY, VOL. 10, 542–562 (1997)

NUCLEOPHILIC ADDITION VERSUS ELECTRON TRANSFER IN CARBONYLMETALLATE SALTS. DONOR–ACCEPTOR INTERACTIONS IN THE PRECURSOR ION PAIRS†

T. MICHAEL BOCKMAN AND JAY K. KOCHI*

Department of Chemistry, University of Houston, Houston, Texas 77204-5641, USA

The isostructural pentacarbonylmetallate anions $M(CO)_5^-$ (M = Mn and Re) react with a series of *N*-methylpyridinium cations (Py^+) to yield products of nucleophilic addition [NA = Py–$M(CO)_5$] or of one-electron redox reaction [ET = $Py^{\bullet} + M(CO)_5^{\bullet}$]. The partitioning of the reaction along the two reaction pathways is controlled by steric factors and the electronic structure of the pyridinium cation, with cations which form stable, delocalized radicals favoring the ET pathway. The central metal also plays a role in determining the stoichiometry, and the NA pathway is favored by the rhenate anion and ET by the manganate analogue. Rates of both reactions correlate with the driving force for electron transfer, and the differing reaction pathways are not distinguished on the basis of linear free energy relations, previously discussed by Bordwell and co-workers. The contact ion pair [Py^+, $M(CO)_5^-$] is identified as the critical precursor for both electron transfer and nucleophilic coupling. Based on these observations, it is proposed that the rates and mechanisms of these interionic reactions are controlled by donor–acceptor bonding in the transition states, which in turn is directly related to the charge-transfer interactions extant in the ion-pair intermediate. © 1997 John Wiley & Sons, Ltd.

J. Phys. Org. Chem. **10**, 542–562 (1997) No. of Figures: 7 No. of Tables: 4 No. of References: 67

Keywords: nucleophilic addition; electron transfer; carbonylmetallate salts; donor–acceptor interactions

Received 30 September 1996; revised 27 January 1997; accepted 31 January 1997

INTRODUCTION

The nucleophilic reactivity of electron-rich organic molecules in addition and substitution reactions is generally correlated with their thermodynamic one-electron redox potentials. Thus, good nucleophiles tend to be good reducing agents. This qualitative observation has been rigorously formulated in quantitative terms by Bordwell and co-workers,[1, 2] who have shown that the same linear free-energy relation (the Brønsted equation) pertains both to a wide variety of two-electron nucleophilic reactions and to single electron transfers. As a result, the attention of physical organic chemists has been focused on the intimate relationship between electron transfer and nucleophilic reactivity, and the problem is currently pursued on both experimental[3, 4] and theoretical[5–10] levels. Our interest in this question centers on the consequences, in chemical terms, of this mechanistic duality, and how the closely related processes of nucleophilic addition and electron transfer lead to different outcomes.

The interconnection between nucleophilicity and electron transfer has been particularly noted in the reactions of carbonylmetallate anions,[11] which are highly reactive nucleophiles,[12, 13] (indeed, they are considered to be 'supernucleophiles'[12]) as well as easily oxidized electron donors.[14, 15] These anions are examples of 'soft' nucleophiles (with high-lying HOMOs),[6] which are known to participate in both (two-electron) addition/substitutions and electron transfers.[16–20] Our interest is particularly drawn to the anions $Re(CO)_5^-$ and $Mn(CO)_5^-$, which forms an isostructural pair of donors.[21] Both are electron rich, with comparable oxidation potentials of $-0{\cdot}26$ and $-0{\cdot}14$ V vs SCE, respectively.[22] Carbonylrhenate and -manganate anions have also been identified as nucleophiles in a variety of addition and substitution reactions.[23, 24] We chose the series of *N*-methylpyridinium cations (Py^+) to serve as both electrophiles and electron acceptors.[25–27] The electrophilic reactivity and thermodynamic redox potentials of these cations can be readily tuned by merely varying the substituents on the pyridinium ring. Moreover, the reactions of the negatively charged nucleophiles with cationic electrophiles can be modulated by solvent polarity and by

† Dedicated to Fred Bordwell for his seminal contributions to our understanding of nucleophilic reactivity.

* *Correspondence to:* J. K. Kochi.

Contract grant sponsor: National Science Foundation.
Contract grant sponsor: Robert A. Welch Foundation.
Contract grant sponsor: Texas Advanced Research Program.

 CCC 0894–3230/97/070542–21 $17.50

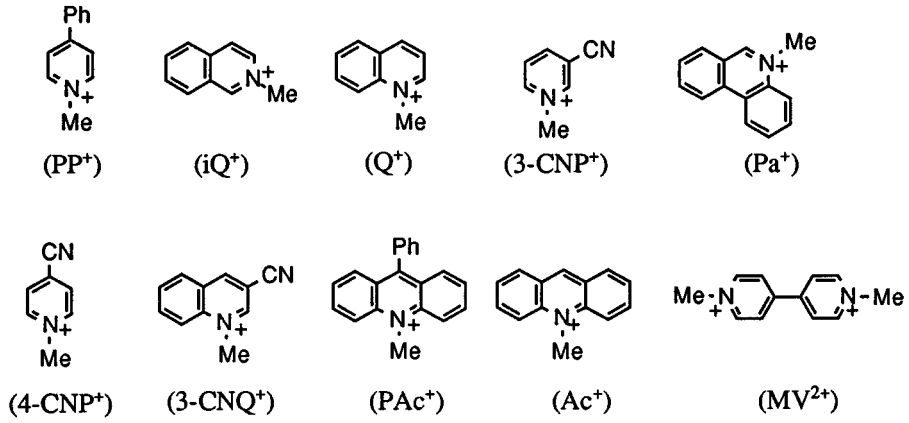

Chart 1

added salt, both of which control the pre-association of the ions.[28–32] By these means, the specific interionic interactions within the intermediate ion pair can be examined. Accordingly, we wish to show how the study of nucleophilic and electron-transfer processes in pyridinium/carbonylmetallate ion pairs will shed new light on the general mechanism of nucleophilic reactions.

RESULTS

Addition and electron-transfer reactions of $Re(CO)_5^-$ with pyridinium acceptors

Pentacarbonylrhenate with N-methylacridinium cations

The addition of 1 equiv. of *N*-methylacridinium trifluoromethanesulfonate to an acetonitrile solution of $Re(CO)_5^-$ [as the bis(triphenylphosphine)iminium or PPN^+ salt] led to an immediate reaction as the pale yellow solution of the rhenate salt became bright orange. The infrared spectrum of the reaction mixture showed that the carbonyl bands of the rhenium anion at ν_{CO} = 1916 and 1861 cm^{-1} [33] had disappeared and were replaced by new bands at 2126, 2045, 2011 and 1985 cm^{-1}. A small amount of white solid precipitated at the same time. Removal of the solvent followed by extraction of the residue with diethyl ether afforded an orange solid, which was identified as 9-(*N*-methylacridanyl)pentacarbonylrhenium(I) by comparison of its IR spectrum with that of (η^1-cycloheptatrienyl)pentacarbonylrhenium(I),[34] and the identity of this product was confirmed by x-ray crystallography (see below). The adduct was formed in 90% yield as determined by quantitative infrared analysis of the reaction mixture. The reaction was thus identified as the cation/anion combination of the pentacarbonylrhenate anion with the electrophilic *N*-methylacridinium cation by a process which we designate hereafter as *nucleophilic addition*, i.e.

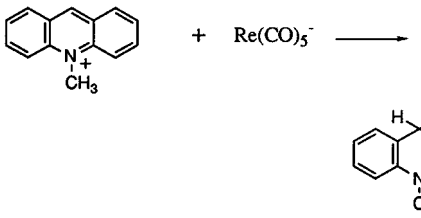

(1)

The white precipitate was identified as *N*,*N*′-dimethyl-9,9′-biacridanyl on the basis of its ^1H NMR spectrum, and it was formed in 6% yield. A small amount of $Re_2(CO)_{10}$ [5% based on $Re(CO)_5^-$] was also detected and quantified by its infrared absorption band at 2070 cm^{-1}.

The ORTEP view of the nucleophilic adduct in Figure 1 shows the rhenium pentacarbonyl moiety as a distorted square pyramid, with the two equatorial carbonyl groups on

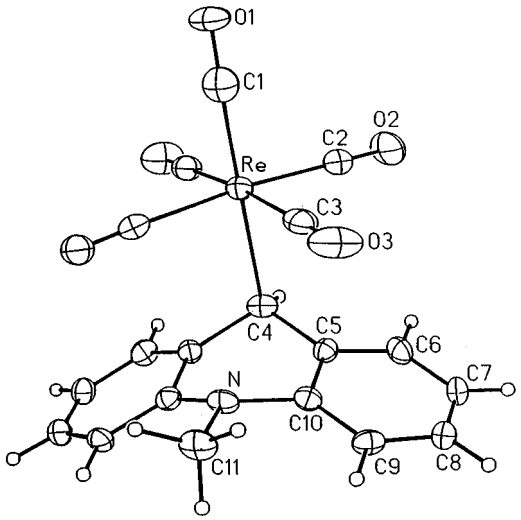

Figure 1. ORTEP view of the adduct formed from *N*-methylacridinium cation and rhenium pentacarbonyl anion

the side of the acridanyl moiety bent towards the axial carbonyl group. The rhenium–carbon bond length is essentially the same as that present in the corresponding cycloheptatrienyl complex. (2·362 vs 2·348 Å).[34] The acridanyl group has a folded structure, with a 137° dihedral angle between the planar aromatic rings. The carbon attached to rhenium is sp^3-hybridized, with C–C–C and Re–C–C bond angles of 111° and 109°.

The UV–VIS absorption spectrum of the nucleophilic adduct, Ac–$Re(CO)_5$, revealed a band with $\lambda_{max}=414$ nm and $\varepsilon_{max}=1000\ l\ mol^{-1}\ cm^{-1}$ which was responsible for its orange color in solutions. The carbonyl infrared spectrum of the nucleophilic adduct in acetonitrile or tetrahydrofuran showed four bands at $\nu_{CO}=2126$, 2045, 2014 and 1985 cm^{-1}. The high-energy band (2126 cm^{-1}) was characteristic of alkylrhenium pentacarbonyl complexes,[35] and was assigned to the fully symmetric (A_1) vibrational stretch. [The observation of four bands, rather than the three expected for a square pyramidal geometry[35] probably derived from the small deviation from idealized C_{4v} symmetry of the $Re(CO)_5$ group, as shown by the x-ray structure.] The nucleophilic adduct decomposed upon heating in benzene at 80 °C to form dirhenium decarbonyl and *N*,*N*′-dimethyl-9,9′-biacridanyl in 70 and 91% yield, respectively, i.e.

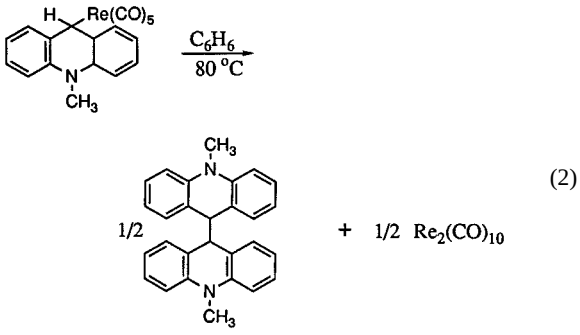

(2)

In contrast to the immediate formation of the rhenium adduct from *N*-methylacridinium, the corresponding 9-phenyl-*N*-methylacridinium cation yielded only the dimeric $Re_2(CO)_{10}$ and the persistent 9-phenyl-*N*-methylacridanyl radical,[36] in quantitative yield, according to the equation

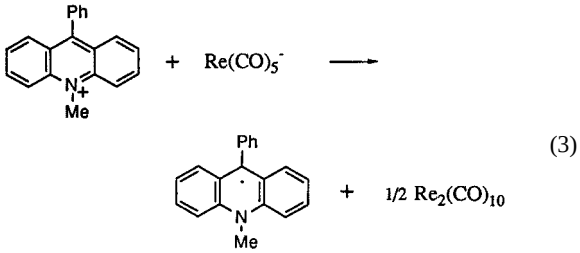

(3)

Since the acridanyl radical and $Re_2(CO)_{10}$ were the unambiguous products of one-electron oxidation and reduction of the cation[36] and anion,[14] respectively, the transformation in equation (3) was designated as *electron transfer*.

Reaction of $Re(CO)_5^-$ with other pyridinium cationic acceptors

Other *N*-methylpyridinium cations reacted with pentacarbonylrhenate to yield the products of addition or electron transfer. For example, solutions of $PPN^+Re(CO)_5^-$ turned bright orange upon addition of the triflate salts of 3-cyano-*N*-methylquinolinium (3-CNQ^+), *N*-methylphenanthridinium (Pa^+), 3-cyano-*N*-methylpyridinium (3-CNP^+), *N*-methylquinolinium (Q^+) and *N*-methylisoquinolinium (iQ^+) to indicate formation of the nucleophilic adducts in Table 1. Thus, upon addition of 3-CNP^+OTf^- to a tetrahydrofuran solution of $PPN^+Re(CO)_5^-$ the carbonyl absorption bands of the rhenate anion were replaced by the diagnostic carbonyl bands of the nucleophilic adduct with $\nu_{CO}=2120$, 2036, 2010 and 1979 cm^{-1}. The solution showed the characteristic orange color and visible absorption band of the adduct ($\lambda_{max}=454$ nm). The nucleophilic adduct did not persist, and its IR spectral bands disappeared concomitantly with the growth of the carbonyl bands of $Re_2(CO)_{10}$ at 2070 and 2006 cm^{-1} (see Table 2).

The formation of the nucleophilic adducts from the *N*-methylquinolinium (Q^+) and *N*-methylisoquinolinium (iQ^+) cations was not quantitative. Thus, the addition of Q^+OTf^- to the rhenate solution caused only a partial (50%) diminution of the IR bands of $Re(CO)_5^-$. The visible band of the nucleophilic adduct ($\lambda_{max}=454$ nm) and the characteristic IR absorbances at $\nu_{CO}=2117$, 2039, 2009 and 1973 cm^{-1} were observed, but these decayed as the bands of $Re_2(CO)_{10}$ grew in. The temporal diminution of the infrared absorption at 2117 cm^{-1} and the visible band in the electronic spectrum both followed first-order kinetics, with $k_{obs}=2{\cdot}8\times10^{-3}\ s^{-1}$ (see Figure 2). The carbonyl infrared bands of the corresponding isoquinolinyl adduct formed from iQ^+OTf^- and $PPN^+Re(CO)_5^-$ could not be observed. Instead, a high yield of the oxidative dimer, $Re_2(CO)_{10}$, was obtained together with minor amounts of an unidentified carbonyl-containing species with $\nu_{CO}=2030$ and 1947 cm^{-1}. A band assigned to the nucleophilic adduct ($\lambda_{max}=460$ nm) was transiently observed in the visible spectrum, but it decayed on the same time-scale ($\tau_{1/2}\approx2$ h) as the disappearance of the infrared bands of $Re(CO)_5^-$ with $\nu_{CO}=1914$ and 1861 cm^{-1}. The latter coincided with the growth of the carbonyl bands of dimeric $Re_2(CO)_{10}$.

Other pyridinium cations did not show spectral evidence for the formation of the nucleophilic adduct. Thus the 4-phenylpyridinium cation reacted slowly (50% conversion after 48 h) with $Re(CO)_5^-$ in tetrahydrofuran. Dirhenium decacarbonyl was the only observed product, and it was formed quantitatively. No orange color or spectral band at 450 nm band (characteristic of nucleophilic adducts) was observed in the solution. Similarly, 1 equiv. of the ditriflate salt of methylviologen reacted instantly with $Re(CO)_5^-$ in acetonitrile to yield a dark blue solution of the methylviolo-

Table 1. Electron-transfer and nucleophilic addition reactions of pyridinium cations with pentacarbonylrhenate[a]

	Nucleophilic addition			Electron transfer	
Pyridinium acceptor	λ_{max}[b] (nm)	ν_{co}[c] (cm^{-1})	Yield[d] (%)	$Re_2(CO)_{10}$[e] (%)	$Py^{\cdot}$[f] (%)
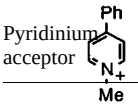	g		0	100	—[h]
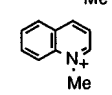	460	—[i]	—[i]	0	0
	454	2117	97[j]	<5	—[h]
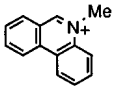	446	2120	80	0	—[h]
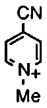	432	2111	95	5	—[h]
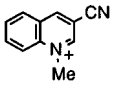	—[g]		0	40	—[h]
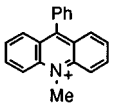	420	2126	100	0	—[h]
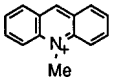	—[g]		0	100	100[k]
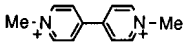	414[l]	2126	95	5	6
	—[g]			73	78

[a] Conducted at 20 °C in tetrahydrofuran by mixing equimolar $5{\cdot}0\times10^{-3}$ M solutions of $[PPN^+]$ $[Re(CO)_5^-]$ and the pyridinium cation as the triflate salt.
[b] Visible absorption maximum of the pyridinium–$Re(CO)_5$ adduct.
[c] Highest energy (A_1) carbonyl IR band of the adduct.
[d] Yield of the adduct, assessed by infrared spectroscopy at ν_{CO} immediately after mixing of the reagents.
[e] Yield of $Re_2(CO)_{10}$.
[f] Yield of the pyridinyl dimer.
[g] Adduct not observed.
[h] Pyridinyl dimer too unstable to quantify.
[i] Infrared band too weak to observe.
[j] For 58% conversion of $Re(CO)_5^-$.
[k] Assayed by UV–VIS spectroscopy of the stable pyridinyl radical.
[l] In acetonitrile.

gen cation radical ($MV^{+\bullet}$), the product of one-electron reduction. The accompanying oxidative dimer, dirhenium decacarbonyl, was formed in 78% yield.

Addition and electron-transfer reactions of $Mn(CO)_5^-$ with pyridinium acceptors

Upon the addition of 1 equiv. of *N*-methylacridinium triflate to a solution of $PPN^+Mn(CO)_5^-$ in acetonitrile, a white solid immediately precipitated. Infrared analysis of the supernatant solution showed that the carbonyl IR bands of $Mn(CO)_5^-$ at $\nu_{CO}=1894$ and 1861 cm^{-1} had been replaced by the characteristic bands of dimanganese decacarbonyl (at $\nu_{CO}=2047$, 2012 and 1981 cm^{-1}). Analysis of the reaction mixture, as detailed in the Experimental section, showed that $Mn_2(CO)_{10}$ was formed in quantitative yield. The white solid that precipitated was collected and identified as *N*,*N*′-dimethyl-9,9′-biacridanyl by comparison of its ^1H NMR spectrum with that of the authentic dimer synthesized previously.[37] The acridanyl dimer could be isolated in 86% yield, and the stoichiometry of the reaction was thus identified as the electron-transfer process in the equation

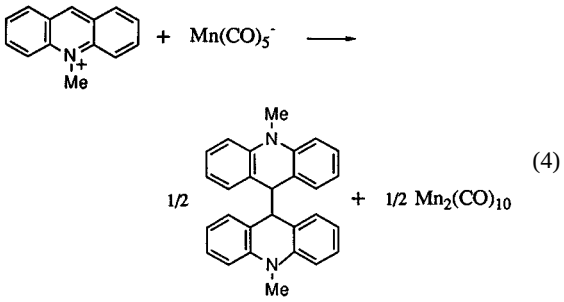

(4)

A transient red color was observed during the reaction. The UV–VIS spectrum of the reaction mixture disclosed a new band $\lambda_{max}=520$ nm which was responsible for the color.

Table 2. Decomposition of the Py–$Re(CO)_5$ Adducts[a]

Py	$t_{1/2}$[b] (s)	Temperature (°C)	ΔG^{*}[c] (kcal mol^{-1})	Products (%) $Re_2(CO)_{10}$	Products (%) Py–Py
—				81	
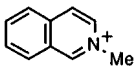	$3{\cdot}5\times10^2$	20	21	73	
	$3{\cdot}5\times10^2$	20	21	58	
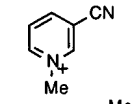	$2{\cdot}7\times10^3$[d]	60	25	48	
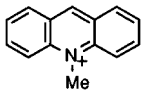	$3{\cdot}6\times10^3$[d, e]	80	27	75	91

[a] Conducted on the nucleophilic adducts generated *in situ* from Py^+OTf^- and $PPN^+Re(CO)_5^-$ unless noted otherwise.
[b] half-life of the transient adducts.
[c] Calculated as $\Delta G^{*}=2{\cdot}3\,RT[13-\log(\ln 2/t_{1\text{-}2})]$.
[d] Decomposition of the isolated adducts.
[e] In benzene solution.

This band formed immediately upon addition of the acridinium cation to the solution of $PPN^+Mn(CO)_5^-$, and it decayed to the spectral baseline within 5 min. On the basis of the similarity of this band to those of the rhenium adducts, the transient band was assigned to the transient adduct $Ac–Mn(CO)_5$. Unfortunately, the concentration of the nucleophilic adduct in the red solution was too low to observe its characteristic carbonyl bands in the infrared spectrum, which showed only the bands of the predominent product, the dimeric $Mn_2(CO)_{10}$.

In contrast to the instantaneous reaction of *N*-methylacridinium with the carbonylmanganate anion, *N*-methylisoquinolinium cation reacted rather slugggishly. The infrared bands of $Mn(CO)_5^-$ diminished over the course of several hours. The manganese dimer was obtained in quantitative yield. Evaporation of the solvent and extraction of $Mn_2(CO)_{10}$ and PPN^+OTf^- with ethanol left a tan residue, which was identified as *N*,*N*′-dimethyl-1,1′-biisoquinolinyl by comparison of its ^1H NMR spectrum with that of the authentic dimer.[38] A 90% yield of biisoquinolinyl was determined by ^1H NMR spectroscopy of the crude reaction mixture using 1,2-dichloroethane as internal standard. Since the biisoquinolinyl dimer was previously established as the product of electrochemical reduction of the N-methyl isoquinolinium cation, the complete stoichiometry of the reaction was thus established as the electron transfer in the equation

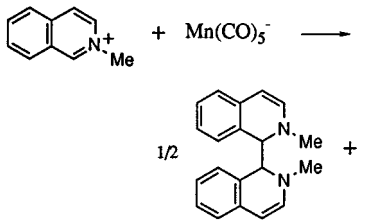

(5)

The redox reactions of $Mn(CO)_5^-$ with a series of *N*-methylpyridinium cations were examined in tetrahydrofuran solution. The course of the reaction was followed by simultaneously monitoring the diminution of the carbonyl infrared bands of $Mn(CO)_5^-$ and the growth of those of $Mn_2(CO)_{10}$. The rate of the reaction was found to be highly dependent on the pyridinium acceptor (see Table 3), and the reaction times ranged from several days for 4-phenyl-*N*-methylpyridinium to a few seconds for 3-cyano-*N*-methylquinolinium. In each case, $Mn_2(CO)_{10}$ was formed in greater than 90% yield. It is noteworthy that a transient red–brown color appeared upon addition of the pyridinium salt to the solution of $Mn(CO)_5^-$, and it bleached during the reaction (see below).

The kinetics of the reaction could not be fitted unambiguously to either a simple first- or second-order rate law.

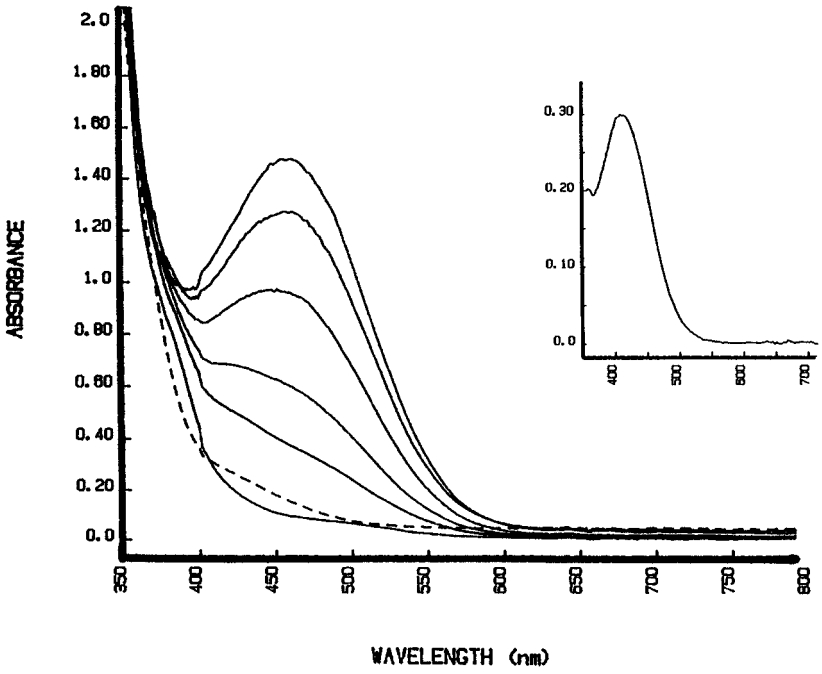

Figure 2. UV–VIS spectra of the adduct formed from *N*-methylquinolinium cation and $Re(CO)_5^-$ in tetrahydrofuran. The dotted line is the spectrum of $Re(CO)_5^-$ (as the PPN^+ salt) in the absence of the quinolinium acceptor. The inset shows the visible absorption band of the stable *N*-methylacridinyl–$Re(CO)_5$ adduct

Table 3. Nucleophilic addition and electron transfer reactions of the pyridinium cationic acceptors with pentacarbonylmanganate[a]

	Addition	Electron transfer		
Pyridinium acceptor	λ_{max}[b] (nm)	k_1[c] (s^{-1})	$Mn_2(CO)_{10}$[d] (%)	Py[e] (%)
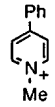	—[f]	3×10^{-6}	100	—[g]
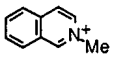	—[f]	$7{\cdot}0\times10^{-5}$	100	91
	—[f]	$3{\cdot}8\times10^{-4}$[h]	100	
	—[f]	$7{\cdot}3\times10^{-4}$[i]	100	—
	—[f]	$1{\cdot}7\times10^{-3}$[j]	97[k]	—
	—[f]	Fast[l]	96[m]	100
	—[f]	$3{\cdot}0\times10^{-4}$	94	—[g]
	—[f]	$1{\cdot}4\times10^{-3}$	91	—[g]
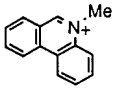	—[f]	$6{\cdot}7\times10^{-3}$	92	—[g]
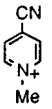	—[f]	$1{\cdot}2\times10^{-2}$	100	—[g]
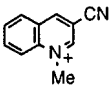	—[f]	$1{\cdot}1\times10^{-1}$	90	—[g]
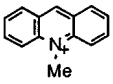	520		95	90

[a] Conducted at 20 °C in tetrahydrofuran by mixing $5{\cdot}0\times10^{-3}$ M solutions of $[PPN^+][Mn(CO)_5^-]$ and the pyridinium acceptor as the triflate salt.
[b] Absorption band maximum of the transient adduct.
[c] Rate constant for ion-pair collapse of $[Py^+, Mn(CO)_5^-]$ ion pairs.
[d] Yield of $Mn_2(CO)_{10}$, based on $Mn(CO)_5^-$ conversion.
[e] Yield of reduced pyridinium cation, as the dimer, Py–Py.
[f] Adduct not oberved.
[g] Dimer too unstable to quantify.
[h] At 50 °C.
[i] At 60 °C.
[j] Same as entry 2, except with $PPN^+Mn(CO)_4P(OPh)_3^-$.
[k] $Mn_2(CO)_8[P(OPh)_3]_2$.
[l] Too fast to measure with $PPN^+Mn(CO)_4PPh_3^-$.
[m] $Mn_2(CO)_8(PPh_3)_2$.

Typically, the reaction followed first-order kinetics for approximately one half-life and then gradually slowed. We tentatively ascribe this mixed kinetics to the incursion of an ionic exchange, such as that presented in Scheme 1, which reduced the concentration of the reactive $[Py^+, Mn(CO)_5^-]$ ion pair.

$$[PPN^+Mn(CO)_5^-] + [Py^+OTf^-] \overset{K_{ex}}{\rightleftharpoons} [PPN^+OTf^-] + [Py^+Mn(CO)_5^-] \quad (6)$$

$$[Py^+Mn(CO)_5^-] \xrightarrow{k_1} Py^{\bullet} + Mn(CO)_5^{\bullet} \quad (7)$$

Scheme 1

Such an ion-pair exchange was consistent with the marked decrease in the reaction rate upon addition of the inert salt tetra-*n*-butylammonium perchlorate to the reaction mixture. Thus, the reaction of 3-cyanoquinolinium with $Mn(CO)_5^-$ was too fast to measure in pure tetrahydrofuran, but required several minutes for completion if 4 equiv. of $TBA^+ClO_4^-$ were present. Indeed, the kinetic equations based on the mechanism in Scheme 1 could be solved in closed form under the assumption that K_{ex} in equation (6) was unity, i.e. that the ions associated indiscriminately (see the Experimental section). The first-order rate constants (k_1) for the electron transfer in equation (7) are listed in Table 3.

Pre-equilibrium formation of charge-transfer ion pairs as the precursors to nucleophilic addition and electron transfer

The reactions of the $M(CO)_5^-$ nucleophiles with the pyridinium cations were marked by a series of characteristic color changes as both the electron-transfer and nucleophilic addition reactions proceeded. For example, the addition of colorless *N*-methylisoquinolinium triflate $[iQ^+][OTf^-]$ to a solution of $[PPN^+][Mn(CO)_5^-]$ was attended by an immediate color change from pale yellow to red–brown. As the redox reaction proceeded, the color of the solution gradually faded to yellow. Similar color changes could also be observed upon addition of either 4-phenyl-*N*-methylpyridinium (PP^+) or *N*-methylphenanthridinium (Pa^+) triflate to solutions of the $Mn(CO)_5^-$ in tetrahydrofuran. In each case, an inspection of the UV–VIS spectra of the solution revealed the source of the initial color to be a new visible absorption band, which is shown in Figure 3 for the case of the isoquinolinium cation. The intensity of this band diminished markedly upon addition of 1 equiv. of the inert salt tetra-*n*-butylammonium perchlorate ($TBA^+ClO_4^-$), as shown in the inset in Figure 3. Since the absorption band did not correspond to the local transitions of either *N*-methylisoquinolinium or of $Mn(CO)_5^-$, the new band was attributed to the charge-transfer absorption of the ion pair, $[iQ^+, Mn(CO)_5^-]$. As such, the diminution of the band intensity upon addition of inert salt could thus be explained

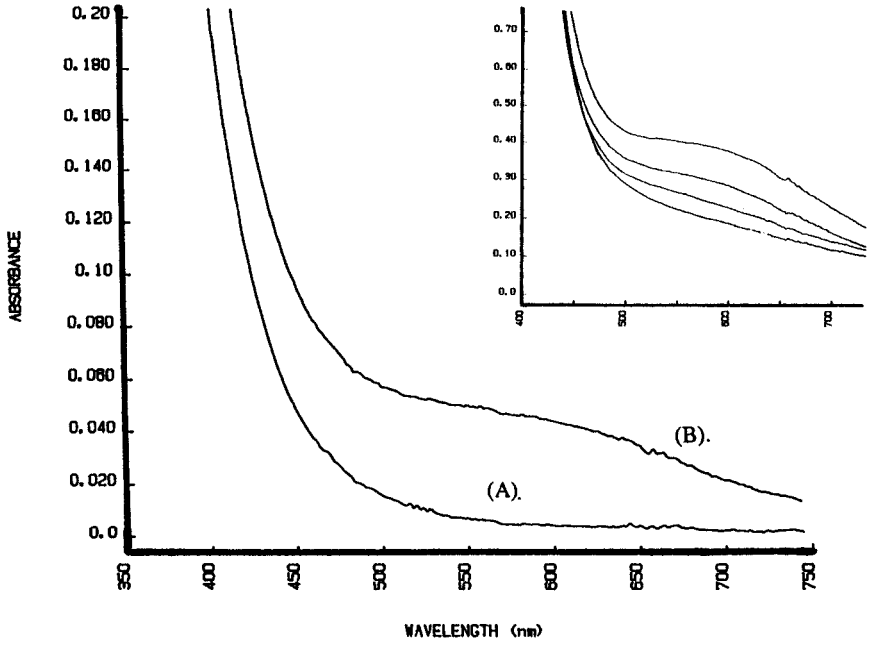

Figure 3. Visible absorption spectrum of $Mn(CO)_5^-$ in tetrahydrofuran as (A) the PPN^+ salt alone and (B) upon addition of 1 equiv. of *N*-methylisoquinolinium triflate. The inset shows the decrease in the visible absorption band upon addition of 1, 2 and 4 equiv. of tetra-*n*-butylammonium perchlorate

Table 4. Charge-transfer bands of pyridinium cationic acceptors with $Re(CO)_5$ and $Mn(CO)_5^-$ [a]

		$Mn(CO)_5^-$		$Re(CO)_5^-$	
Pyridinium acceptor	E^0_{red} (V vs SCE)[b]	λ_{CT}[c] (nm)	$\Delta\nu$[d] (cm^{-1})	λ_{CT} (nm)	$\Delta\nu$ (cm^{-1})
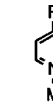	1·20[e]	560	6000	580	6000
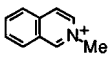	1·15[f]	580	6100	630	5300
	0·96[f]	640	5900	—[g]	
	0·82[f]	—[g]	—[g]		
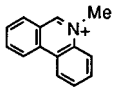	0·78[f]	670		—[g]	
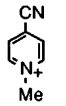	0·67[h]	—[g]	—[g]		
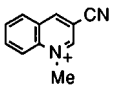	0·53[f]	—[g]	—[g]		
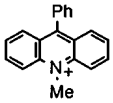	0·52[i]	—[g]	—[g]		
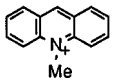	0·46[j]	—[g]	—[g]		
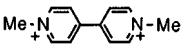	0·42[k]	—[g]	—[g]		

[a] Determined by UV–VIS spectroscopy of equimolar solutions (0·01 M) of $[PPN^+]$ $[Mn(CO)_5^-]$ and pyridinium triflate in tetrahydrofuran.
[b] Thermodynamic reduction potentials of the pyridinium cations in acetonitrile.
[c] Charge-transfer band maximum (±15 nm).
[d] Width at half maximum of the CT band.
[e] Reversible E_0^{red} from Ref. 49.
[f] Corrected for dimerization.
[g] Rapid redox or addition reaction. Reversible E_0^{red} from Refs [h]50, [i]35, [j]66 and [k]48b.

by the ion-pair exchange, i.e.

$$[iQ^+][Mn(CO)_5^-]+[TBA^+][ClO_4^-] \rightleftharpoons [iQ^+][ClO_4^-]+[TBA^+][Mn(CO)_5^-] \quad (8)$$

The progressive red shift of the band maximum for the pyridinium carbonylmanganate ion pairs in Table 4 followed the trend in the reduction potentials of the pyridinium cations (E^0_{red}) in the order $PP^+ < iQ^+ < Pa^+$. Such a variation of the band maximum with the redox potential is characteristic of charge-transfer (λ_{CT}) absorptions,[39] and the new absorption in the visible was thus assigned to the charge-transfer transition ($h\nu_{CT}$), i.e.

$$[iQ^+, Mn(CO)_5^-] \xrightarrow{h\nu_{CT}} [iQ^{\bullet}, Mn(CO)_5^{\bullet}] \quad (9)$$

The CT bands of all the pyridinium/carbonylmetallate ion pairs were characteristically broad,[28, 31] as shown by their spectral widths (FWHM) ranging from 5300 to 7000 cm^{-1} in Table 4. (The broad diffuse nature of the bands accounted for the dull brownish colors of solutions of the CT salts.) The charge-transfer absorption bands of the manganese and rhenium pentacarbonyl anions paired with more strongly oxidizing cations, such as that of *N*-methylacridinium in Tables 1 and 3, could not be observed, owing to rapid reactions between the pyridinium acceptors and $M(CO)_5^-$ in equations (1) and (4).

In the case of the reaction of $Re(CO)_5^-$ with *N*-methylisoquinolinium, the charge-transfer ion pair and the nucleophilic adduct were observed simultaneously. The charge-transfer band of the ion pair appeared as a broad tail (inset, Figure 4), with $\lambda_{CT} = 630$ nm, while the visible absorption band of the adduct appeared with a well resolved maximum ($\lambda_{max} = 460$ nm). Upon addition of $TBA^+ClO_4^-$ to the solution, the charge-transfer band and the band of the adduct both diminished in intensity, as shown in Figure 4.

Photostimulation of the charge-transfer ion pairs

The Mulliken formulation in equation (9) predicts that the electron-transfer reactions of the ion pairs can be induced by photoexcitation of their charge-transfer absorption bands. This effect was investigated for the *N*-methylisoquinolinium (iQ^+) and 4-phenyl-*N*-methylpyridinium (PP^+) ions paired with the carbonylmanganate anion. Thus, the irradiation of a solution of $[iQ^+, Mn(CO)_5^-]$ with light filtered to excite only the charge-transfer band in Figure 3 resulted in quantitative oxidation of $Mn(CO)_5^-$ to $Mn_2(CO)_{10}$. [This irradiation was carried out at low temperatures (0 °C), at which the thermal reaction was too slow to occur.] Precisely the same behavior was observed upon the irradiation of the charge-transfer bands of the $[PP^+, Mn(CO)_5^-]$ ion pair.

The photostimulated redox process was also investigated by time-resolved spectroscopic methods. Thus, the irradiation of the charge-transfer band of $[iQ^+, Mn(CO)_5^-]$ with the second harmonic (532 nm) of an Nd:YAG laser gave rise to the transient spectra observed in Figure 5. The broad band at $\lambda_{max} = 760$ nm was identified as the carbonylmanga-

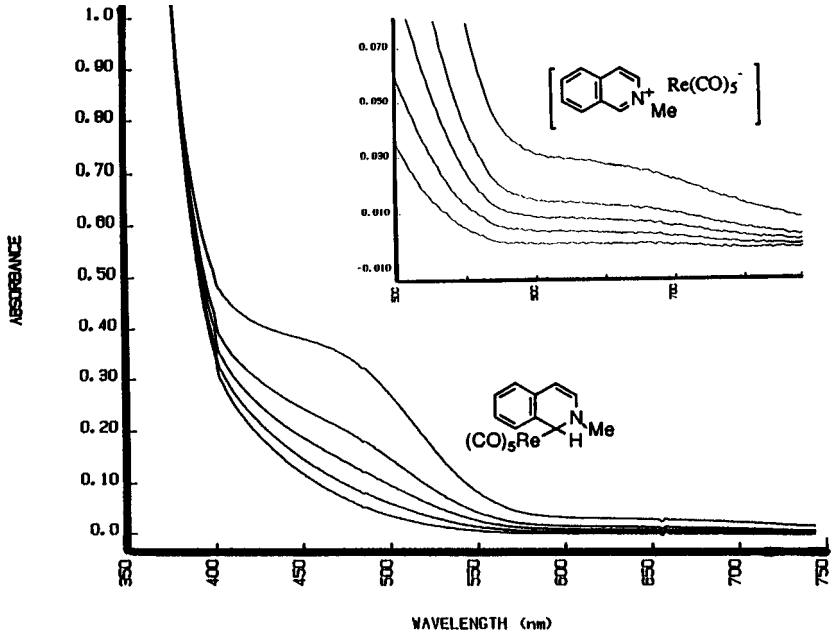

Figure 4. Decrease of the visible band of the adduct iQ–$Re(CO)_5$ upon addition of the inert salt tetra-*n*-butylammonium perchlorate. The inset shows the accompanying decrease in the charge-transfer band of the $[iQ^+, Re(CO)_5^-]$ ion pair

nese radical, $Mn(CO)_5^{\cdot}$, by comparison of the absorption band with that of the pentacarbonylmanganese radical previously generated by flash photolysis.[40, 41] This species decayed on the early microsecond time-scale, and a new absorbance at 540 nm grew in simultaneously. The same growth of a 540 nm band and decay of $Mn(CO)_5^{\cdot}$ was observed upon the irradiation of the charge-transfer band of $[PP^+, Mn(CO)_5^-]$. On the other hand, irradiation of the corresponding cobalticenium/$Mn(CO)_5^-$ ion pair generated $Mn(CO)_5^{\cdot}$, which simply decayed to baseline and did not form any other transient species.

DISCUSSION

The behaviors of the carbonylmetallate anions in Tables 1 and 3 indicate that $Mn(CO)_5^-$ and $Re(CO)_5^-$ can react both as nucleophiles and as electron donors. For example, $Re(CO)_5^-$ reacts with the *N*-methylacridinium cation (Ac^+) to yield the adduct, Ac–$Re(CO)_5$, by nucleophile–electrophile coupling. The rhenium carbonyl anion thus acts as a typical nucleophile, and the nucleophilic addition in equation (1) compares with the analogous additions of hydroxide (pseudo-base formation),[42, 43] Grignard reagents,[44] hydride[45] and other nucleophiles[46] to substituted pyridinium cations. On the other hand, the reaction of $Re(CO)_5^-$ with 9-phenyl-*N*-methylacridinium cation yields only $Re_2(CO)_{10}$ and the 9-phenyl-*N*-methylacridanyl radical by a process of electron transfer. The contrasting behavior for $Re(CO)_5^-$ with the two closely related acridinium cations indicates that subtle changes in the conditions of the reaction can control the chemical outcome. Accordingly, let us first identify those structural factors that favor one reaction mode over another. The mechanistic significance of the close relationship between electron transfer and nucleophilic addition will then be considered. Finally, the role of the precursor ion pair $[Py^+, M(CO)_5^-]$ will be taken into account.

Influence of the pyridinium moiety

The nucleophilic adducts become increasingly stable to homolytic cleavage [compare equation (2)] in the order isoquinolinyl < quinolinyl < phenanthridanyl < acridanyl (see Table 2). This order follows the trend in the redox potentials (E^0_{red}) of the pyridinium cations in Table 4. For the least electrophilic cation, *N*-methylisoquinolinium (iQ^+), the ion pair is formed together with the nucleophilic adduct, as spectrally demonstrated by the simultaneous appearance of the band of the nucleophilic adduct (at $\lambda_{max} = 460$ nm)[47] and

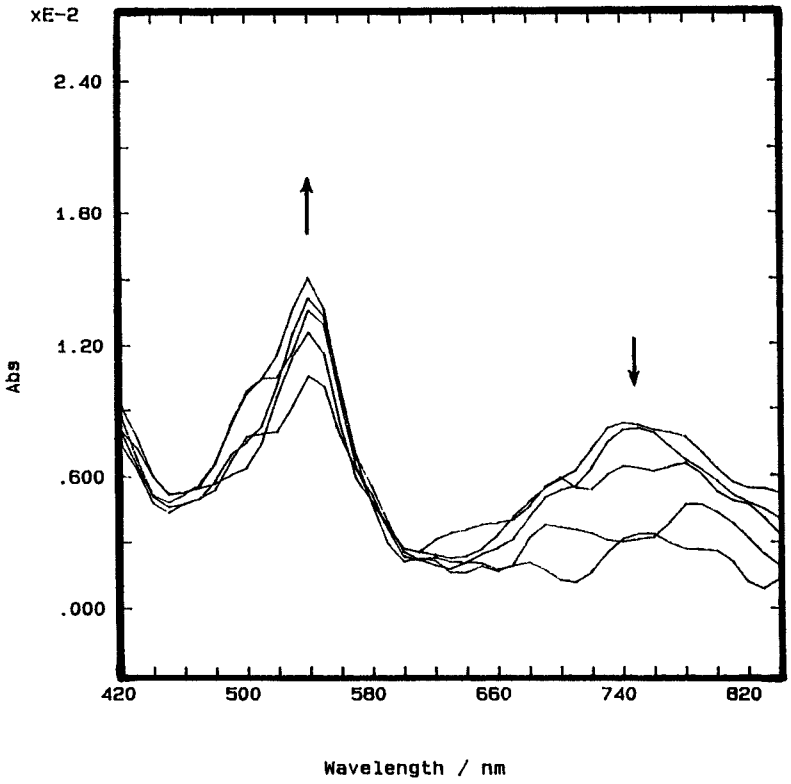

Figure 5. Time-resolved visible spectra recorded following the charge-transfer irradiation of the $[iQ^+, Mn(CO)_5^-]$ ion pair

the charge-transfer band of the ion pair (λ_{CT} = 630 nm) in Figure 4. The spectral intensities of the two bands indicate that the adduct and the ion pair constitute the principal products in the reaction mixture. Since the addition of inert salt leads to a decrease in the intensity of the spectral bands of both the adduct and the ion pair in Figure 4, we conclude that these exist in coupled equilibria involving ion-pair exchange and nucleophilic addition, according to the equation

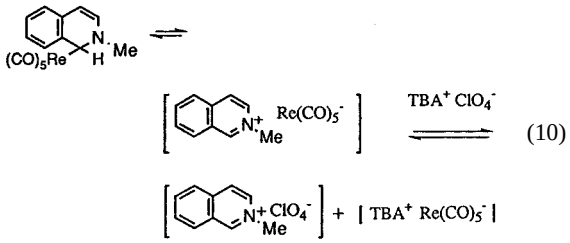

(10)

By contrast, the spectral band of the more stable *N*-methylacridanyl adduct, Ac–Re(CO)$_5$, is not affected by added salt. We conclude that the isoquinolinyl nucleophilic adduct is destabilized with respect both to salt-induced heterolytic cleavage in equation (10) and to homolytic cleavage in Table 2, as compared with its *N*-methylacridanyl analogue. We believe that the comparative stability of the adducts in both processes reflects the increasing Re–C bond strength for the adducts formed from the more electrophilic pyridinium cations. According to this view, as the adducts become more stable, the reaction changes from an overall electron transfer process to a nucleophilic addition and the cleavage of the adduct becomes increasingly less important.

At the other end of the scale, there are pyridinium cations which do not form nucleophilic adducts with $Re(CO)_5^-$ (see entries 1, 6, 8 and 10 in Table 1). These are cations that are reduced to persistent pyridinyl radicals, which are stabilized by delocalization of the radical center over multiple aromatic rings (e.g. the reduced form of methylviologen) or steric encumbrance of radical coupling by substituents (e.g. *N*-methyl-4-cyanopyridinyl). The frustration to nucleophilic addition of these pyridinium cations reflects a combination of steric hindrance to coupling (disfavoring nucleophilic addition) and stabilization of the pyridinyl radical products (which favors the alternative electron-transfer pathway). In this context, it should be noted that these same factors which inhibit adduct formation also inhibit dimerization of the pyridinyl radicals. As a result, the reductions of the cations which do not form adducts are electrochemically reversible on the cyclic voltammetric time-scale.[38, 48–50]

Effect of the central metal

The anions $Mn(CO)_5^-$ [51] and $Re(CO)_5^-$ [52] are isostructural, with an essentially identical trigonal bipyramidal arrangement of carbonyl ligands around the central metal. Yet these two anions appear distinctly different in their reactivity towards pyridinium acceptors. The manganese anion reacts in all cases by electron transfer, and a (transient) adduct is observed only in the reaction with *N*-methylacridinium. On the other hand, the rhenium counterpart with *N*-methylpyridinium cations readily forms a series of nucleophilic adducts of varying (homolytic) stability. The enhanced stability of the rhenium adducts (compared with their manganese analogues) reflects the greater dissociation energy of the Re–C versus the Mn–C bond. For example, the dissociation energy of the methyl–rhenium bond in $CH_3Re(CO)_5$ is greater than that of the corresponding bond in $CH_3Mn(CO)_5$ by about 16 kcal mol^{-1} (1 kcal = 4·184 kJ).[53, 54] As a measure of the bond energies of the various rhenium adducts, the activation energies (ΔG^*) for decomposition of the adducts are given in Table 2. Since these values fall between 20 and 30 kcal mol^{-1}, the bond energies of the corresponding manganese adducts, if reduced by the same difference, would lie in the range 4–14 kcal mol^{-1}. Thus the manganese adducts, if formed, are expected to be transient. In line with this computation, the *N*-methylacridanyl/rhenium adduct is the most stable, and the corresponding Mn adduct can be observed as a transient. [Note that the η^1-cycloheptatrienyl complex of $Re(CO)_5$ is stable and isolable under conditions in which the corresponding complex of $Mn(CO)_5$ cannot be observed.[34] The manganese complex is persistent, however, in a low-temperature matrix.[55]]

We conclude that the effects of the pyridinium moiety (Py) and the central metal (M) on the partitioning between electron transfer and nucleophilic addition is determined by the varying strength of the metal–carbon bonds in the nucleophilic adducts Py–M(CO)$_5$. According to this formulation, the nucleophilic adducts formed between $Re(CO)_5^-$ and electrophilic cations are stable to both homolytic cleavage in Table 2 and heterolysis in equation (10), and thus can be observed and characterized. On the other hand, steric effects, or the substitution of manganate for rhenate, implies weakened Py–M bonding, and the reaction proceeds by electron transfer.

Interpretations of concurrent nucleophilic/electron-transfer reactivity

The isolation and characterization of persistent pyridinyl/pentacarbonylrhenium adducts raises the question of the involvement of σ-bonded intermediates in the simple redox transformations of $Re(CO)_5^-$ and $Mn(CO)_5^-$. In other words, the electron transfer may be effected without proceeding through an intermediate, i.e.

$$Py^+Mn(CO)_5^- \rightarrow Py^{\bullet} + Mn(CO)_5^{\bullet} \qquad (11)$$

followed by dimerization of the radicals to give the ultimate redox products. Alernatively, a two-step (inner-sphere)[8, 9] sequence of bond formation and bond homolysis may effect the same transformation:

$$Py^+Mn(CO)_5^- \rightarrow Py{-}Mn(CO)_5 \qquad (12)$$

$$Py–Mn(CO)_5 \rightarrow Py^{\bullet} + Mn(CO)_5^{\bullet} \quad (13)$$

The latter process has been identified in the reactions of $Re(CO)_5^-$ with pyridinium cations as well as metal carbonyl anions with organometallic cationic acceptors such as $M(CO)_6^+$ (M = Mn, Re)[18] and $LFe(CO)_3^+$ (L = η^5-pentadienyl).[17] The reaction of $Mn(CO)_5^-$ with pyridinium acceptors, however, appears at first glance to be a simple electron transfer. For example, the rates of the redox reactions in Table 3 increase smoothly as the reduction potential (E^0_{red}) of the cationic donors becomes more positive. This dependence relates directly to the energy gap, $\Delta G_{ET} = F(E^0_{red} + E^0_{ox})$ for electron transfer in equation (11). However, since increasing E^0_{red} correlates with the increasing electron deficiency of the pyridinium cations, it also relates to their electrophilicities, and the addition of anionic nucleophiles to a series of cationic electrophiles obeys the same linear free energy relation,[1,2] i.e. $\Delta G^* = \beta \Delta G_{ET} + \text{constant}$. Note, for example, that the activation energy for the reaction of iQ^+ with $Re(CO)_5^-$ falls on the line in the plot in Figure 6 even though the reaction is one of nucleophilic addition. Moreover, the slope of the ΔG^* vs ΔG_{ET} plot (β) is only 0·36, which is substantially less than the value of unity expected for outer-sphere electron transfer.[56] These results are in line with the extensive data available for organic nucleophile–electrophile coupling reactions, which show a general correlation with the thermodynamics of electron transfer.[1,2] The alternative formulation of the redox reactions of $Mn(CO)_5^-$ and $Re(CO)_5^-$ in terms of the inner-sphere reaction in equations (12) and (13) runs into problems when the kinetic stability of the Re and Mn adducts is considered. Thus, the lifetimes of the adducts of $M(CO)_5^-$ with *N*-methylacridinium are longer than can be accounted for under the assumption that the adduct is the intermediate to the radical products. For example, $Re_2(CO)_{10}$ and biacridanyl are formed immediately upon reaction of *N*-methylacridinium and $Re(CO)_5^-$ although the adduct is stable for hours. Similarly, the transient adduct formed from *N*-methylacridinium and $Mn(CO)_5^-$ decomposes steadily over 20 min, but the redox reaction to form biacridanyl and $Mn_2(CO)_{10}$ is essentially complete upon mixing of the substrates. These facts demonstrate that nucleophilic addition does not precede electron transfer. Thus, the resolution of the mechanistic ambiguity must lie in the identification of the intermolecular interactions which occur prior to the rate-limiting steps for the two processes, as follows.

Charge-transfer ion pairs as the initial intermediates

The reaction of oppositely charged ions such as Py^+ and $M(CO)_5^-$ is preceded by an ion-pairing step. In a non-polar solvent such as tetrahydrofuran, the ion pairs (and their higher aggregates) are the only charged species present, and the cation—anion annihilation reaction proceeds via first-order collapse of the ion pair. For the [Py^+, $M(CO)_5^-$] salts, the electronic interaction between the ions leads to a partial transfer of charge from the anion to the cation, which is

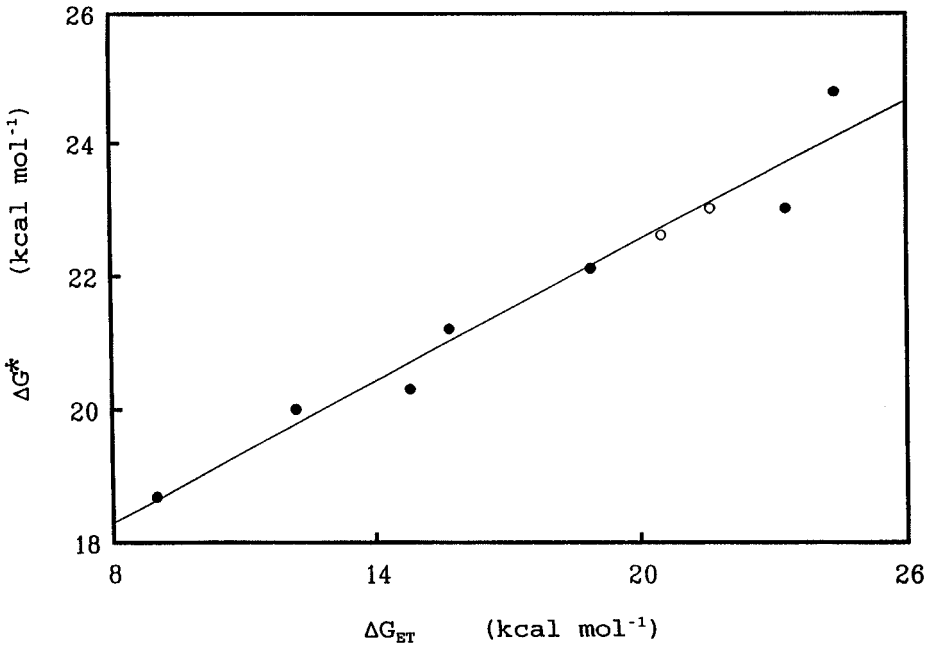

Figure 6. Linear free energy relationship between the activation energies for the reactions of pyridinium cations with either $Mn(CO)_5^-$ (closed circles) or $Re(CO)_5^-$, plotted against the driving force for interionic electron transfer. The linear slope has a value of 0·36

directly observable as the charge-transfer (CT) band of the ion pair. In a molecular orbital sense, this corresponds to a partial bonding interaction between the LUMO of the pyridinium acceptor and the HOMO of the carbonylmetallate donor. Since this frontier MO overlap is critical to nucleophilic addition as well as to electron transfer, the interionic CT interaction may play a role in the transition state for both reactions. Thus, the decreasing charge-transfer energy gap ($h\nu_{CT}$) in Figure 7 correlates with both an increasingly exergonic driving force ($-\Delta G_{ET}$) for electron transfer, and with an increasing rate for the redox and nucleophilic addition reactions in Figure 6. Note that the points for the pyridinium cation/rhenate and manganate ion pairs in Figure 7 lie on the same line and are not separately distinguished.

The association of redox products with adducts in Table 1 (entries 5 and 9) indicates that these concurrent processes are closely related, with transition states that are structurally and energetically similar. The idea that the transition state for the redox reaction involves incipient bond formation (and thus strongly resembles the transition state for nucleophilic attack) is supported by the large negative entropy of activation (-46 cal mol^{-1} K^{-1}) in Table 3 for the formation of the redox products from the [iQ$^+$, Mn(CO)$_5^-$] ion pair. On the other hand, the charge-transfer interaction in the [iQ$^+$, Re(CO)$_5^-$] analogue points to partial electron transfer in the transition state for the nucleophilic addition. To shed light on this mechanistic conundrum, we induce the direct electron transfer by photostimulation of the charge-transfer band of the ion pair.

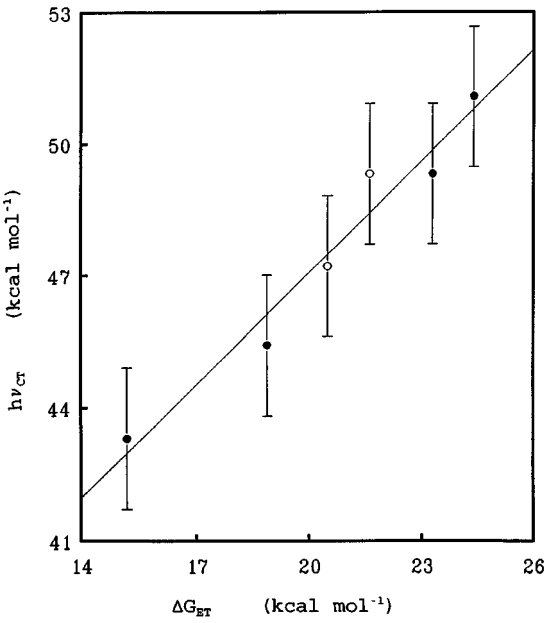

Figure 7. Mulliken plot of the energies of the charge-transfer bands of the [Py$^+$M(CO)$_5^-$] ion pairs as a function of the driving force for electron transfer. The closed and open circles indicate manganate and rhenate ion pairs, respectively, and the error bars represent the uncertainty of the measurement

Direct electron transfer from the manganate donor to the pyridinium cations is effected by the irradiation of the charge-transfer band of the [Py$^+$, Mn(CO)$_5^-$] ion pair, and the short-lived intermediates can be observed by time-resolved spectroscopy. Irradiation of the CT ion pairs from [Mn(CO)$_5^-$] paired with [iQ$^+$] or [PP$^+$] cations forms the radical Mn(CO)$_5^{\bullet}$, identified by its long-wavelength absorption centered at $\lambda_{max}=760$ nm. This signal decays, and a new species is formed with $\lambda_{max}=520$ nm. This band is identical with the absorption band of the transient adduct formed from Mn(CO)$_5^-$ and *N*-methylacridinium and may be compared with the absorption bands (414–460 nm) of the stable rhenium adducts. As such it is assigned to the transient adduct of Py$^{\bullet}$ and Mn(CO)$_5^{\bullet}$ formed by radical–radical combination, i.e. as shown in Scheme 2.

$$Py^+ Mn(CO)_5^- \xrightarrow{h\nu_{CT}} Py^{\bullet} + Mn(CO)_5^{\bullet}$$

$$Py^{\bullet} + Mn(CO)_5^{\bullet} \rightarrow Py - Mn(CO)_5$$

Scheme 2

Since the Mn adducts have weak bonds (see above), decomposition of the adducts is favored, and ultimately only the redox products are observed. Nevertheless, Scheme 2 illustrates how electron transfer can lead to an overall nucleophilic addition to the pyridinium cation.

Both the nucleophilic addition and electron-transfer reactions require structural changes of the M(CO)$_5^-$ anion. The transient radicals, M(CO)$_5^{\bullet}$, do not have the trigonal bipyramidal (D_{3h}) geometry of the anions. Instead, their structure is square pyramidal (C_{4v}), as established by infrared[57] and ESR[58] studies. Since the disposition of the carbonyl groups in the adducts is also square pyramidal (see Figure 1), the same reorganizational changes in nuclear structure accompany either electron transfer or nucleophilic addition in which the cation-induced distortion of the anion induces a geometry change to one characteristic of both the M(CO)$_5^{\bullet}$ radical and the Py—M(CO)$_5$ nucleophilic adduct. This geometric distortion is present to a degree even in the precursor ion pairs, as established by structural studies in the solid state and in solution.[21] The distorted anion is thus activated towards either reaction pathway. In other words, the transition states for electron transfer and nucleophilic addition are close in both structure and energetics, so that bond formation will crucially affect the outcome of the reaction. It should be noted that structural alteration of a donor or acceptor towards the geometry of its reduced or oxidized form plays a central role in the Marcus theory of electron transfer, where it relates to the reorganization energy.[59] In this context, the broadness of the charge-transfer bands of the intermediate CT ion pairs also reflects a large reorganization energy associated with the change in the geometry of the metallate upon oxidation.[60] The close relationship between electron transfer and nucleophilic

reactivity has been taken into account by several theoretical treatments, which explicitly invoke a degree of charge transfer in the transition states for nucleophilic addition and substitution.[5–7] The latter also point to transition states for structurally coupled electron transfer and charge-transfer nucleophilic addition that are closely linked.

CONCLUSIONS

The linear free energy relationship between the driving force for electron transfer from $Re(CO)_5^-$ and $Mn(CO)_5^-$, and their reaction rates for nucleophilic addition and electron transfer indicate that the transition states for the two reactions are closely related. In accordance with this view, carbonylmetallate anions, $M(CO)_5^-$, can react with pyridinium electrophiles (Py^+) either by electron transfer [to yield $Py^\bullet$ and $M(CO)_5^\bullet$ radicals] or by nucleophilic addition [to yield the Py—$M(CO)_5$ adducts]. The course of the reaction depends critically on the pyridinium cation and on the central metal of the carbonylmetallate. Nucleophilic attack is favored by pyridinium cations which allow steric accessibility of the incoming nucleophile to the pyridinium ring. Electron transfer is facilitated if the pyridinium cation is sterically hindered or if the radical center is stabilized by delocalization. Both reactions proceed via the intermediate [Py^+, $M(CO)_5^-$] ion pair, and the interaction between the HOMO of the metallate donor and the LUMO of the pyridinium acceptor is visibly manifested as a charge-transfer electronic transition. The interplay of the two reaction modes at the mechanistic border suggests that this charge-transfer bonding interaction is critical to both nucleophilic and electron-transfer reactivity. Indeed, the most economical explanation to accommodate all of our results is to invoke a rate-limiting electron transfer within the precursor (CT) ion pair as a common step to both processes. We hope that further detailed comparisons of the thermal (adiabatic) and charge-transfer (non-adiabatic) activation of the precursor ion pair, as preliminarily described in Figure 5, will help to clarify further the precise role of electron role in nucleophilic processes.

EXPERIMENTAL

Materials. The metal carbonyl dimers $Mn_2(CO)_{10}$ and $Re_2(CO)_{10}$ from Pressure Chemical were used as received. Bis(triphenylphosphine)iminium chloride, [PPN]Cl, was prepared by the method of Ruff and Schlienz.[61] Methyl trifluoromethanesulfonate (methyl triflate) was obtained from Aldrich and used as received. The pyridine bases quinoline and isoquinoline (Fischer) were distilled before use. Acridine (Aldrich) was recrystallized from ethanol. Phenanthridine, 3-cyanoquinoline, 4-phenylpyridine (Aldrich), 4-cyanopyridine and 3-cyanopyridine (Reilly Tar and Chemical) were used as received. The pyridinium acceptors were all prepared as their trifluoromethanesulfonate (triflate) salts. Typically, a solution of methyl triflate (1·65 g; 10 mmol) in 10 ml of dichloromethane was added to a solution of 10 mmol of the pyridine base in 10 ml of the same solvent. After the exothermic reaction subsided, diethyl ether (150 ml) was added to precipitate the pyridinium salt. The resulting crude trifluoromethanesulfonate salts were collected and recrystallized from a mixture of acetonitrile and ethyl acetate. 4-Phenyl-*N*-methylpyridinium triflate: 2·70 g (84%). ^{1}H NMR (CD_3CN): δ 8·62 (d, J=6·8 Hz, 2H), 8·24 (d, J=6·6 Hz, 2H) 7·88–7·99 (m, 2H), 7·61–7·68 (m, 3H), 4·28 (s, 3H). IR (KBr): 3129, 3059, 1650, 1566, 1494, 1475, 1441, 1266 (vs, OTf), 1225, 1169, 1150, 1031, 856, 775, 722, 697, 638, 575, 550, 519, 488 cm^{-1}. *N*-Methylisoquinolinium triflate: 2·50 g (87%). ^{1}H NMR (CD_3CN): δ 9·54 (s, 1H), 7·92–8·45 (m, 6H), 4·93 (s, 3H). IR (KBr): 3059, 1656, 1609, 1522, 1478, 1397, 1266 (OTf) 1225, 1153, 1031, 878, 762, 712, 637, 571, 516, 472 cm^{-1}. Anal. Calculated for $C_{11}H_{10}F_3NO_3S$: C, 45·05; H, 3·44; N, 4·78. Found: C, 44·93; H, 3·48; N, 4·72%.*N*-Methylquinolinium triflate: 2·55 g (88%). ^{1}H NMR (CD_3CN): δ 9·04–9·12 (m, 1H) 7·91—8·42 (m, 6H) 4·56 (s, 3H). IR (KBr): 3100, 3059, 1629, 1606, 1594, 1531, 1468, 1455, 1424, 1386, 1371, 1353, 1272 (OTf), 1224, 1160, 1140, 879, 834, 777, 754, 747, 636, 571, 517, 488, 464 cm^{-1}. Anal. Calculated for $C_{11}H_{10}F_3NO_3S$: C, 45·05; H, 3·44; N, 4·78. Found: C, 45·13; H, 3·48; N, 4·75%. 3-Cyano-*N*-methylpyridinium triflate: 2·05 g (73%). ^{1}H NMR (CD_3CN): δ 9·12 (s, 1H), 8·83 (br t, 2H), 8·16 (br, t, 1H), 4·35 (s, 3H). IR (KBr): 3160, 3086, 2253 (w, CN), 1641, 1572, 1475, 1269 (OTf), 1181, 1137, 1028, 828, 759, 672, 638, 575, 519 cm^{-1}. Anal. Calculated for $C_8H_7F_3N_2O_3S$: C, 35·83; H, 2·63; N, 10·44. Found: C, 35·88; H, 2·58; N, 10·36%. *N*-methylphenanthridinium triflate: 2·30 g (67%). ^{1}H NMR (CD_3CN): δ 9·76 (s, 1H), 8·90–9·05 (m, 2H), 8·01–8·54 (m, 6H), 4·68 (s, 3H). IR (KBr): 3090, 3031, 1634, 1534, 1512, 1459, 1262, 1166, 1028, 772, 759, 718, 638, 572, 519, 490 cm^{-1}. Anal. Calculated for $C_{15}H_{12}F_3NO_3S$: C, 52·48; H, 3·52; N: 4·08. Found: C, 51·96; H, 3·59; N, 4·04%. 4-Cyano-*N*-methylpyridinium triflate: 2·33 g (87%) ^{1}H NMR (CD_3CN): δ 8·86 (d, J=6·5 Hz, 2H), 8·32 (br s, 2H), 4·37 (s, 3H). IR (KBr): 3125, 3062, 2250 (vw, CN), 1641, 1569, 1519, 1475, 1269 (vs, OTf), 1228, 1172, 1141, 859, 756, 644, 575, 533, 519 cm^{-1}. Anal. Calculated for $C_8H_7F_3N_2O_3S$: C, 35·83; H, 2·63; N, 10·44. Found: C, 35·83; H, 2·63; N, 10·37%. 3-Cyano-*N*-methylquinolinium triflate: ^{1}H NMR (CD_3CN): δ 9·51 (s, 2H), 8·42–8·55 (m, 3H), 8·05–8·22 (m, 1H), 4·62 (s, 3H). IR (KBr): 3047, 2281, 2250 (w, CN), 1634, 1600, 1581, 1522, 1462, 1384, 1353, 1259 (vs, OTf), 1169, 1028, 897, 875, 784, 756, 640, 634, 575, 519, 440 cm^{-1}. *N*-methylacridinium triflate:[62] 3·0 g (86%) bright yellow plates. ^{1}H NMR (CD_3CN): δ 9·87 (s, 1H), 8·28–8·62 (m, 6H), 7·87–8·05 (m, 2H) 4·76 (s, 3H). IR (KBr): 3109, 3058, 3031, 1625, 1528, 1543, 1460, 1395, 1262 (vs, OTf) 1226, 1189, 1154, 1031, 989, 859, 833, 776, 750, 638, 602, 573, 517, 503 cm^{-1}. 9-Phenyl-*N*-methylacridinium triflate:[63] 3·5 g (82%) yellow rhombs. ^{1}H NMR (CD_3CN): δ 8·29–8·68 (m, 4H), 7·50–8·07 (m, 9H), 4·84 (s, 3H). IR (KBr): 3110, 3060, 1611, 1578, 1551, 1457, 1444, 1376, 1264 (vs, OTf), 1223, 1150, 1030, 765, 706, 660, 636, 572, 515 cm^{-1}.

The PPN^+ salt of $Mn(CO)_5^-$ was prepared using the procedure of Faltynek and Wrighton.[64] Typically, a suspension of 1% sodium amalgam (50 g) and tetrahydrofuran (30 ml) was stirred under an atmosphere of argon as $Mn_2(CO)_{10}$ (1·95 g, 5·0 mmol) was added in one portion. The mixture was stirred for 2 h as the initially orange–yellow solution became greenish gray. The solution was filtered through a bed of Celite using a Schlenk frit. To the filtered solution of $Na[Mn(CO)_5]$ in tetrahydrofuran was added [PPN]Cl (5·67 g, 10 mmol) and the mixture was stirred overnight. The orange–yellow solution was filtered through a bed of Celite to remove the white residue of NaCl, and overlayed by 150 ml of diethyl ether. The solution was allowed to stand for 2 days at −25 °C, and it deposited bright yellow plates of $[PPN^+][Mn(CO)_5^-]$. Yield: 5·3 g (76%). IR (ν_{CO}, tetrahydrofuran): 1894 (vs), 1861 (vs) cm^{-1}. Lit.: 1894, 1861 cm^{-1}. The PPN^+ salt of $Re(CO)_5^-$ was prepared from $Re_2(CO)_{10}$ and $[PPN^+][Cl^-]$.[13] Yield: 5·0 g (59%). IR (ν_{CO}, tetrahydrofuran): 1916 (vs), 1861 (vs) cm^{-1}, Lit.: 1914, 1860 cm^{-1}. The substituted carbonylmanganese dimers, $Mn_2(CO)_8(PPh_3)_2$ and $Mn_2(CO)_8[P(OPh)_3]_2$, were prepared by the reaction of $Mn_2(CO)_{10}$ with PPh_3 or $P(OPh)_3$ in refluxing *n*-butanol.[65] $Mn_2(CO)_8(PPh_3)_2$: IR (ν_{CO}, $CHCl_3$) 1985 (w), 1955 (vs) cm^{-1}. Lit.:[65] 1985, 1955 cm^{-1}. $Mn_2(CO)_8[P(OPh)_3]_2$: IR (ν_{CO}, $CHCl_3$) 2003 (w), 1978 (vs) cm^{-1}. Lit.:[65] 2003, 1978 cm^{-1}. The substituted carbonylmanganate salts $[PPN^+][Mn(CO)_4PPh_3^-]$[64] and $[PPN^+][Mn(CO)_4P(OPh)_3^-]$[14] were prepared by literature methods. $[PPN^+][Mn(CO)_4PPh_3^-]$: IR (ν_{CO}, tetrahydrofuran) 1914, 1846, 1814 cm^{-1}. Lit.: 1939, 1838, 1816 cm^{-1}. $[PPN^+][Mn(CO)_4P(OPh)_3^-]$: IR ($\nu_{CO}$, tetrahydrofuran) 1961, 1869, 1841 cm^{-1}.

Tetrahydrofuran (THF, Fisher) was distilled serially from potassium hydroxide and lithium aluminum hydride under an argon atmosphere, and then transferred to a Schlenk flask under an inert atmosphere of argon for storage. Acetonitrile (Fisher) was stirred with 0·1 wt% $KMnO_4$ for 24 h, and the mixture was refluxed until the liquid was colorless. The solvent was decanted from the brown MnO_2 residue and distilled from phosphorus pentoxide under an argon atmosphere. After a final distillation from CaH_2, the acetonitrile was transferred to a Schlenk flask under an argon atmosphere. Diethyl ether was distilled under an atmosphere of argon from lithium aluminum hydride. All solvents were stored in Schlenk flasks under a positive pressure of argon.

*Instrumentation.*The UV–VIS absorption spectra were recorded on a Hewlett-Packard Model 8450A diode-array spectrometer. The ^1H NMR spectra were recorded on a JEOL FX 90-Q spectrometer, and chemical shifts are reported in ppm units downfield from tetramethylsilane. IR spectra were recorded on a Nicolet 10DX FT spectrometer with the aid of 0·1 mm NaCl cells.

The nanosecond and microsecond time-resolved spectral measurements were carried out with a Q-switched Nd:YAG laser (Quantel YG 580-10) and a kinetic spectrometer consisting of a 150 W xenon arc lamp, an Oriel 77250 150 mm monochromator and a detector consisting of a photomultiplier (Hamamatsu R928) interfaced to a Tektronix 7104 oscilloscope and a Tektrix C1001 digitizing camera. Data acquisition was controlled by a sequence generator, laser controller and backoff unit from Kinetic Instruments. The data were stored and analyzed by ASYST programs running on a Gateway 2000 personal computer. The laser source for the picosecond time-resolved transient spectral measurements was a mode-locked Nd:YAG laser (Quantel YG 501-C). Excitation was carried out using the second or third harmonic (532 or 355 nm). The excitation beam traversed a variable delay stage (up to 4·5 ns) before being directed on to the sample cuvette. Analyzing light was provided by a continuum beam generated by directing the residual fundamental light (1064 nm) into a 10 cm cuvette containing a 50:50 mixture of H_2O and D_2O. The collimated white light was split into two directions by means of a neutral density filter as a semi-transparent mirror. One beam was directed into the sample cuvette overlapping with the excitation beam to probe the excited sample, while the other served as reference. The sample and reference beams were collected by fiber optic cables and led to a monochromator (Instruments SA HR-320). The signal was recorded on a dual diode array (Princeton Instruments DD-512) that was calibrated with the 436 and 546 nm lines from a mercury lamp.

The steady-state photolyses were carried out with the focused beam from a 500 W high-pressure Hg lamp. The beam was passed through a water filter and an appropriate glass cut-off filter (Corning CS series) to remove infrared and ultraviolet light. The sample was contained in a Pyrex Schlenk tube immersed in a room temperature water-bath.

Reactions of pyridinium acceptors with pentacarbonylrhenate $Re(CO)_5^-$

9-(N-Methylacridanyl)pentacarbonylrhenium(I). A solution of $[PPN^+][Re(CO)_5^-]$ (0·506 g, 0·58 mmol) in 20 ml of acetonitrile was stirred and cooled in a dry ice–acetone bath. When the solvent began to freeze (−30 °C) solid *N*-methylacridinium triflate (0·20 g, 0·585 mmol) was added and the solution was warmed to −5 °C. The yellow solution turned bright orange as the acridinium salt dissolved. The solution was allowed to stir at −5 °C for 2 h and then warmed to 20 °C. The infrared spectrum of the reaction mixture showed the complete disappearance of the carbonyl infrared bands of $Re(CO)_5^-$ at ν_{CO}=1916 and 1861 cm^{-1} and the appearance of those belonging to the adduct, Ac–$Re(CO)_5$, at ν_{CO}=2126, 2014 and 1985 cm^{-1}. The cloudy orange solution was filtered to remove a white precipitate, and the acetonitrile solvent was reduced in volume to *ca* 4 ml. An orange precipitate (0·25 g) of the adduct formed. The supernatant was transferred to a Schlenk flask and the solvent was completely removed *in vacuo*. The residue was extracted with diethyl ether, and removal of the solvent from the extracts afforded an

additional 0·045 g of the adduct. The ether-insoluble residue (0·292 g) was identified as $[PPN^+]OTf^-$ (0·43 mmol) by its infrared spectrum. The rhenium adduct (total yield 0·294 g, 90% yield) was recrystallized by dissolution in acetonitrile and cooling to −25 °C to afford orange plates, which were suitable for x-ray structural determination. IR (ν_{CO}, tetrahydrofuran): 2126 (A_1), 2045 (sh), 2014(E), 1985 (A_1) cm^{-1}. ^1H NMR (C_6D_6): δ 6·72–7·20 (m, 6H), 6·60 (d, J=9 Hz, 2H), 4·53 (s, 1H), 2·91 (s, 3H). UV–VIS (THF): λ_{max} (log ε) 414 nm (3·0). The white residue which formed initially was dissolved in $CDCl_3$ and identified as *N*,*N*′-dimethyl-9,9-biacridanyl by comparison of its NMR spectrum with that in the literature.[37] Toluene (5·0 μl) was added and the yield of the acridanyl dimer was determined by integration of the signal of its *N*-methyl protons (δ 2·91) compared with the methyl protons of the toluene internal standard. Yield: 0·018 mmol (6% relative to the acridinium triflate). The carbonyl infrared spectrum of the crude reaction mixture showed a band at 2070 cm^{-1}, which was ascribed to $Re_2(CO)_{10}$. Comparison of its absorbance with that of a standard solution of $Re_2(CO)_{10}$ in the same cell showed that the rhenium dimer was formed in 5% yield.

6-(N-Methylphenanthridanyl)-pentacarbonylrhenium(I). From 0·334 g (0·385 mmol) of $[PPN^+][Re(CO)_5^-]$ and 0·132 g (0·385 mmol) of Pa^+OTf^- was obtained 0·14 g (70%) of red–orange crystals. ^1H NMR (C_6D_6): 7·40–7·66 (m, 2H), 6·75–7·10 (m, 5H), 6·33 (d, J=9 Hz, 1H), 5·29 (s, 1H), 2·38 (s, 3H). IR (ν_{CO}, THF): 2111 (m), 2046 (w), 2003 (vs), 1977 (m) cm^{-1}. UV–VIS: λ_{max} (log ε) 432 nm (3·1).

(3-Cyano-N-methylquinolinyl)pentacarbonylrhenium(I). From 0·357 g (0·413 mmol) of $[PPN^+][Re(CO)_5^-]$ and 0·148 g (0·440 mmol) of $[3\text{-}CNQ^+][OTf^-]$ was obtained 0·12 (56%) brown microcrystals. ^1H NMR (C_6D_6): δ 6·17–6·45 (m, 3H), 5·48 (d, J=10 Hz, 1H), 5·23 (d, J=1 Hz, 1H), 3·52 (s, 1H), 1·90 (s, 3H). IR (νCO, THF): 2126 (m), 2057 (w), 2014 (vs), 1982 (m). UV–VIS: λ_{max} 420 nm. The other adducts were generated *in situ* by addition of the pyridinium triflate salt (0·1 mmol) to a solution of $[PPN^+][Re(CO)_5^-]$ (0·086 mg, 0·10 mmol) in THF (10 ml) and were identified by their infrared (ν_{CO}) and UV–VIS spectra.

(3-Cyano-N-methylpyridinyl)pentacarbonylrhenium(I). IR (ν_{CO}, THF): 2120 (m), 2036 (w sh), 2010 (vs), 1979 (m) cm^{-1}. UV–VIS (THF): λ_{max} 446 nm.

(N-Methylquinolinium)pentacarbonylrhenium(I). IR (ν_{CO}, THF): 2117 (m), 2039 (w sh), 2009 (vs), 1973 (m) cm^{-1}. The yields of the adducts in Table 1 were obtained from their infrared absorbance using the characteristic (A_1) high-energy carbonyl band at 2110–2120 cm^{-1}. The correction factors for all three isolable adducts were the same ($0{\cdot}11 \pm 0{\cdot}01$ mM^{-1}) within experimental error. The same value was assumed for the transient adducts. The yields of $Re_2(CO)_{10}$ in Tables 1 and 2 were obtained by comparison of its infrared absorbance (ν_{CO}=2070 cm^{-1}) with that of a stock solution of the dimer in THF in the same infrared cell.

Thermal decomposition of the carbonylrhenium adducts. *9-(N-methylacridanyl)pentacarbonylrhenium(I).* The adduct (0·022 g, 0·041 mmol) was dissolved in 4·2 ml of benzene in a Schlenk flask and placed in a thermostated oil bath heated to 80 °C. Aliquots of the reaction mixture were removed and analyzed by infrared spectroscopic techniques to monitor the course of the reaction. After 3·5 h, the band of the adduct at 2120 cm^{-1} had disappeared. The yield of $Re_2(CO)_{10}$, assayed at ν_{CO}=2070 cm^{-1}, was 75% based on the adduct. The reaction was repeated without infrared monitoring and after 3·5 h, the reaction mixture was cooled to room temperature and the solvent was removed *in vacuo*. The residue was dissolved in $CDCl_3$, and the ^1H NMR spectrum of the mixture showed only resonances of *N*,*N*′-dimethyl-9,9′-biacridanyl. ^1H NMR ($CDCl_3$): δ 6·70–7·10 (m, 16H), 3·82 (s, 2H), 2·90 (s, 6H). Toluene (10 μl) was added and the yield of the acridanyl dimer was calculated by comparing the integral of the signal from its *N*-methyl protons (δ 2·90) with that from the methyl protons of toluene (δ 2·31).

6-(N-Methylphenanthridinyl)pentacarbonylrhenium(I). Similarly, a solution of this compound (0·017 g, 0·032 mmol) in 3 ml of benzene was placed in an oil bath heated to 60 °C. The reaction was complete after 80 min. Yield of $Re_2(CO)_{10}$: 0·0093 mmol (58%). The other transient adducts were allowed to decompose *in situ* in THF after their formation. Thus the adduct formed from 3-cyano-*N*-methylpyridinium and $Re(CO)_5^-$ decomposed completely within 20 min of its formation to a mixture of $Re_2(CO)_{10}$ (60%) and other (unidentified) rhenium carbonyl products. Similarly the adduct formed from *N*-methylquinolinium and the carbonylrhenate decomposed in the same period to $Re_2(CO)_{10}$ (73%) and other products. The carbonyl infrared spectra were identical in both of these cases, and consisted of the bands of $Re_2(CO)_{10}$ (ν_{CO}=2070 and 2010 cm^{-1}) and unassigned broad bands at 2030 and 1978 cm^{-1}. In the case of *N*-methylquinolinium and $Re(CO)_5^-$, the electronic absorption band of the adduct at λ_{max}=454 nm was monitored during the decomposition. The decay of this band occurred with the same half-life (3·0 min) as that determined by the decay of the 2117 cm^{-1} band of the adduct in the infrared spectrum. In the case of the transient adduct formed from *N*-methylisoquinolinium and $Re(CO)_5^-$, the characteristic band at 2110–2125 cm^{-1} could not be observed. [A very weak and transient band at 2108 cm^{-1} was observed in one run, but it could not be reproduced. The infrared spectrum showed only the decay of the bands of $Re(CO)_5^-$ (ν_{CO}=1906 and 1861 cm^{-1}) and the growth of the bands of $Re_2(CO)_{10}$. The rhenium dimer was formed in 81% yield, and it was accompanied by the unknown rhenium carbonyl products with bands at 2030 and 1978 cm^{-1}. The UV–VIS spectrum of the mixture showed a transient band (λ_{max}=460 nm) assigned to the adduct. The decay of this band in the infrared spectrum occurred on the same timescale ($t_{1/2}$=1 h) as that of the bands of $Re(CO)_5^-$.

Electron-transfer reactions of pentacarbonylrhenate

Re(CO)$_5^-$. Four of the pyridinium cations reacted with $Re(CO)_5^-$ without any evidence for the formation of an adduct. In these cases, no band was observed at 2110–2125 cm^{-1} in the infrared spectrum, and no band was observed in the UV–VIS region between 400 and 500 nm corresponding to the adduct. Thus, 4-phenyl-*N*-methylpyridinium triflate (0·032 g, 0·10 mmol) reacted with $[PPN^+][Re(CO)_5^-]$ (0·082 g, 0·10 mmol) dissolved in 10 ml of THF to yield $Re_2(CO)_{10}$ in quantitative yield, based on 50% conversion of the anion, after 48 h. Similarly, the addition of 4-cyano-*N*-methylpyridinium triflate (0·027 g, 0·10 mmol) to 1 equiv. of $[PPN^+][Re(CO)_5^-]$ in THF yielded a blue, highly air-sensitive solution, and a 40% yield of $Re_2(CO)_{10}$ was estimated on the basis of its carbonyl absorbance at 2070 cm^{-1}. The addition of 9-phenyl-*N*-methylacridinium triflate (0·039 g, 0·10 mmol) to 1 equiv. of $[PPN^+][Re(CO)_5^-]$ in acetonitrile yielded a red solution of the stable *N*-methyl-9-phenylacridanyl radical. The yield of $Re_2(CO)_{10}$ was quantitative and the yield of the radical was 100% based on extinction coefficient ($\varepsilon = 7{\cdot}0\times10^3$ l mol^{-1} cm^{-1}) at 520 nm.[36] Finally, addition of 1 equiv. of methylviologen ditriflate (0·046 g; 0·10 mmol) to a 0·01 M solution of $[PPN^+][ReCO)_5^-]$ in acetonitrile afforded the rhenium dimer in 73% yield.

Electron transfer and addition reactions of pentacarbonylmanganate $Mn(CO)_5^-$. The reaction of $Mn(CO)_5^-$ with the pyridinium cations (as their triflate salts) was conducted as follows: 1 equiv. of the pyridinium triflate was added to a stirred solution of 0·1 mmol of $[PPN^+][Mn(CO)_5^-]$ in 10 ml of THF at 20 °C. The solid immediately dissolved. In the case of the *N*-methylisoquinolinium (iQ^+), *N*-methylquinolinium (Q^+), 3-cyano-*N*-methylpyridinium (3-CNP^+) and *N*-methylphenanthridinium (Pa^+) cations, the formation of the charge-transfer bands of the $[Py^+][Mn(CO)_5]$ ion pairs were observed as transient reddish brown or greenish brown colors. The reactions were followed by observing the growth of the carbonyl infrared bands of $Mn_2(CO)_{10}$ (at υ_{CO} = 2045, 2009 and 1979 cm^{-1}) and the disappearance of the bands of $Mn(CO)_5^-$ (at 1894 and 1861 cm^{-1}). For the reactions of iQ^+ with $Mn(CO)_5^-$ conducted at higher temperatures, a thermostated oil bath was employed as heat source. The yields of $Mn_2(CO)_{10}$ in Table 3 were computed by comparison of the absorbance of the solution at 2045 cm^{-1} (due to the manganese dimer) at the completion of the reaction with the absorbance of the solution at 1894 cm^{-1} $[Mn(CO)_5^-]$ before addition of the pyridinium salt. The relative molar absorbance of the two bands (1·12) was determined by comparing the infrared spectra of stock solutions of $Mn_2(CO)_{10}$ and $[PPN^+][Mn(CO)_5^-]$. The yield of *N*,*N*′-dimethyl-9,9′-bi-acridanyl was determined by ^{1}H NMR analysis using toluene as the internal standard, as described for the decomposition of the rhenium adduct. The yield of *N*,*N*′-dimethyl-1,1′-biisoquinolinyl, $(iQ)_2$,[37] was determined as follows. Upon completion of the reaction, the solvent was removed *in vacuo* and the residue was dissolved in $CDCl_3$. The internal standard (1,2-dichloroethane) was added and the yield of the dimer was determined by combined integrals of its olefinic proton resonances (δ 6·82, 6·32, 6·03 and 5·64 ppm) compared with that of dichloroethane (δ 5·32 ppm).

A transient red color was noted in the reaction of *N*-methylacridinium triflate with $[PPN^+][Mn(CO)_5^-]$ in THF. Examination of the UV–VIS spectrum of the reaction mixture disclosed a new band, with λ_{max} = 520 nm in the visible region of the spectrum. The band decayed to baseline within 5 min following the addition of the acridinium salt to the solution of $Mn(CO)_5^-$. The maximum absorbance of the band, recorded initially, was 0·13.

The rate constants for the reaction of the ion pairs in Table 3 were obtained as follows: the ion-pair equilibrium in Scheme 1 implies that $[Py^+OTf^-]$ $[PPN^+Mn(CO)_5^-] = K_{ex}$ $[PPN^+OTf^-]$. If c is the initial formal concentration of $PPN^+Mn(CO)_5^-$ and Py^+ OTf^- and ζ is the extent of reaction, the equation becomes $[Py^+Mn(CO)_5^-] = (c-\zeta)^2/(2c-\zeta)$.[29] The absorbance of $Mn_2(CO)_{10}$ at 2045 cm^{-1} (a), divided by the final absorbance (a_∞) was taken as the extent of reaction, ζ. This equation then could be integrated as $\ln[a_\infty/(a_\infty - a)] + a\,(a_\infty - a) = k_1 t$. The two terms on the right-hand side of the equation were calculated and the sum plotted as a function of time. The slope of the line was k_1 in Table 3. For the reactions of $Mn(CO)_5^-$ with the 4-cyano-*N*-methylpyridinium (4-CNP^+) and 3-cyano-*N*-methylquinolinium (3-CNQ^+) acceptors, the reaction was too fast to follow by this method. The reactions were conducted in the presence of 4 equiv. of inert salt (tetra-*n*-butylammonium perchlorate). The rate constants were obtained by plotting $\ln[a_\infty/(a_\infty - a)] + 5[a/(a_\infty - a)]$ as a function of time, and equating the slope of the linear relation to k_1.

Electron-transfer reactions of $Mn(CO)_4L^-$, where L = PPh_3 and $P(OPh)_3$. To a solution of $[PPN^+][Mn(CO)_4P(OPh)_3^-]$ ($4{\cdot}9\times10^{-3}$ M) in THF was added 14·4 mg (0·049 mmol) of $[iQ^+][OTf^-]$. The triflate salt dissolved to form a brown solution. The infrared spectrum of the reaction mixture showed the decrease of the carbonyl bands of $Mn(CO)_4P(OPh)_3^-]$ at ν_{CO} = 1961, 1869 and 1841 cm^{-1} and an increase in the strong band of $Mn_2(CO)_8[P(OPh)_3]_2$ at 1979 cm^{-1}. The disubstituted Mn dimer was the only metal carbonyl product (2200–1700 cm^{-1}), and it was formed in practically quantitative yield (0·024 mg, 97%). The rate of the ion pair collapse was determined as described for the reactions with $Mn(CO)_5^-$. This procedure yielded a rate constant of $1{\cdot}7\times10^{-3}$ s^{-1} for the ion-pair collapse in equation (7).

A 1 equiv. amount of $[iQ^+][OTf^-]$ (0·015 g) was added to a solution of $[PPN^+][Mn(CO)_4PPh_3^-]$ ($5{\cdot}2\times10^{-3}$ M) in 10 ml of THF. The reaction mixture was quickly transferred to an infrared cell and the spectrum of the reaction mixture was acquired as rapidly as possible. The bands of $Mn(CO)_4PPh_3^-$ at ν_{CO} = 1939, 1846 and 1814 cm^{-1} diminished as the strong band of $Mn_2(CO)_8(PPh_3)_2$ (1954 cm^{-1}) grew in. The reaction was complete in 6 min, and the yield of the dimer was 0·025 mmol (96%). In a separate

experiment, 0·093 g (0·096 mmol) of [PPN^+][$Mn(CO)_4PPh_3^-$] was allowed to react with 0·029 g (0·098 mmol) [iQ^+][OTf^-]. After 15 min, the solvent was removed *in vacuo* and $CDCl_3$ (1·0 ml) was added to dissolve the residue. Nitromethane (11·5 mg) was added as an internal standard and the integrated resonances of the olefinic protons of the isoquinolinyl dimer (at δ 6·0 and 5·6 ppm) were compared with the signal of the protons of CH_3NO_2 (δ 3·8 ppm). The yield of isoquinolinyl dimer was quantitative (0·049 mmol).

UV–VIS absorption spectra of the ion pairs and the nucleophilic adducts. A tetrahydrofuran solution of [PPN^+][$Mn(CO)_5^-$] and *N*-methylisoquinolinium triflate, each 0·01 M, was transferred to a 1·0 mm cuvette equipped with a Teflon needle valve. The UV–VIS spectrum of the solution was recorded. A 1 equiv. amount of inert salt (tetra-*n*-butylammonium perchlorate, TBAP) was added and the spectrum was recorded again. This procedure was repeated after addition of another 1 equiv. of salt, and the procedure was repeated for the addition of inert salt for a total of 4 and 8 equiv. The nucleophilic adduct, 9-(*N*-methylacridanyl)pentacarbonylrhenium(I), was dissolved in THF to form a 5×10^{-3} M solution and its UV–VIS spectrum was recorded. Inert salt was added incrementally in the amounts of 2, 4, 8 and 20 equiv. of TBAP. The absorbance of the solution at λ_{max} = 414 nm was 1·53 prior to the addition of salt and the successive addition of salt caused it to diminish to 1·51, 1·46, 1·44 and 1·40. Since even the presence of 20 equiv. of TBAP caused only a slight (8%) diminution in the intensity of the absorbance, it was concluded that the effect of added salt on the stable adduct was at most minor.

The charge-transfer spectra of the pyridinium/carbonylmetallate ion pairs were acquired as follows: a stock 0·010 M solution of [PPN^+][$M(CO)_5^-$] (M = Mn or Re) in tetrahydrofuran was transferred to a Schlenk cuvette and the UV–VIS spectrum of the solution was acquired. A 1 equiv. amount of the pyridinium triflate was added and the solution was shaken until the salt dissolved. The absorbance spectrum was then re-recorded. The absorbance of the [PPN^+][$M(CO)_5^-$] was digitally subtracted from the second spectrum, and the maximum of the subtracted spectrum was taken as λ_{max} in Table 4.

Charge-transfer irradiation of the pyridinium/manganate ion pairs.

N-Methylisoquinolinium. A THF solution (7 ml) of [iQ^+][OTf^-] ($6·0\times10^{-3}$ M) and [PPN^+][$Mn(CO)_5^-$] ($5·0\times10^{-3}$ M) was prepared in a Schlenk vessel. A 1·0 ml aliquot was transferred to another Schlenk flask wrapped in aluminum foil to serve as an unirradiated control. Both flasks were placed in an ice–water bath and the first solution was irradiated using a 500 nm cut-off filter (Corning CS) to ensure that photo-stimulation of only the charge-transfer band. The reaction was followed by UV and visible spectroscopy. After 30 min of irradiation, the charge-transfer band of the [iQ^+][$Mn(CO)_5^-$] ion pair had disappeared, and the infrared absorptions of $Mn(CO)_5^-$ were replaced by those of $Mn_2(CO)_{10}$. The yield of the latter was 0·015 mmol (100%) based on the absorbance of the dimer at 2045 cm^{-1}. No change in the infrared spectrum of the unirradiated reaction mixture was observed.

4-Phenyl-N-methylquinolinium. A THF solution (10 ml) of [PP^+][OTf^-] and [PPN^+][$Mn(CO)_5^-$], each $5·0\times10^{-3}$ M, was cooled in an ice–water bath and irradiated with filtered (λ_{irr} > 500 nm) light for 3 h. complete conversion of the manganese anion to $Mn_2(CO)_{10}$ (0·025 mmol, 100%) was observed.

Solutions for time-resolved spectroscopic investigations contained 0·010 M pyridinium triflate and [PPN^+][$Mn(CO)_5^-$] in tetrahydrofuran. The solutions were prepared in Schlenk flasks and were degassed four freeze–pump–thaw cycles. The solution was then transferred to a cuvette for laser irradiation.

The various acceptor cations, A^+ (where A^+ = iQ^+, Q^+, 3-CNP^+, Pa^+ and 3-CNQ^+), were irreversibly reduced on the CV time-scale at a scan rate of 0·5 V s^{-1}. The reversible E^0_{red} values in Table 4 were obtained either from the literature or calculated by accounting for the kinetic potential shift[66] of E_p owing to follow-up dimerization of the radicals, A$^\bullet$, according to the expression $E^0 = E_p + (RT/nF)\times0·905 - (RT/3nF)\ \ln[2/3\ k_{dim}\ C(RT/nFv)]$,[66] where k_{dim} is the second-order rate constant for dimerization of the radicals, C is the concentration of the cation (5×10^{-3} M) and v is the scan rate of 0·5 V s^{-1}. A diffusion-controlled rate of dimerization ($k_{dim} = 2·0\times10^{10}$ M^{-1} s^{-1}) was assumed.[67]

X-ray crystallography of the nucleophilic adduct, 9-(*N*-methylacridanyl)pentacarbonylrhenium(I). An orange slab having approximate dimensions 0·60×0·24×0·12 mm was mounted in a random orientation on a Nicolet R3m/V automatic diffractometer. The radiation used was Mo Kα monochromatized by a highly ordered graphite crystal. Final cell constants, as well as other information pertinent to data collection and refinement are listed as follows: space group, *Pnma*, orthorhombic; cell constants, a = 6·750(1), b = 14·210(2) c = 18·987(3) Å; V = 1821 $Å^3$; molecular formula, $C_{19}H_{12}NO_5Re$; formula weight, 520·52; formula units per cell, Z = 4; density, 1·90 g cm^{-3}; absorption coefficient, μ = 67·9 cm^{-1}; radiation (Mo Kα), λ = 0·71073 Å; collection range, $4\le\theta\le50°$; scan width, $\Delta\theta = 1·40 + (K\alpha_2 - K\alpha_1)$; scan speed range, 2·5–15·0° min^{-1}; total data collected, 1887; independent data [$I > 3\sigma(I)$], 1234; total variables, 128; $R = \Sigma\|F_0| - |F_c\|/\Sigma|F_0|$, 0·036; $R_w = [\sum w\ (|F_0| - |F_c|)^2/\sum w|F_0|^2]^{1/2}$, 0·037; weights, $w = \sigma(F)^{-2}$. The Laue symmetry was determined to be *mmm* and from the systematic absences noted the space group was shown to be either *Pnma* or $Pn2_1a$. Intensities were measured using the omega scan technique, with the scan rate depending on the count obtained in rapid pre-scans of each reflection. Two standard reflections were monitored after every 2 h or every 100 data collected, and these showed no significant variation. Lorentz and polarization corrections were applied, as well as an empirical absorption correction based on psi scans of ten reflections having chi values between 70 and 90°.

Since the molecule is capable of possessing internal symmetry, space group *Pnma* was assumed from the outset. The structure was solved by the use of the SHELXTL direct methods program TREF, which revealed the position of all the nonhydrogen atoms in the asymmetric unit, consisting of one-half molecule situated around a mirror plane. The usual sequence of anisotropic and isotropic refinements was followed, after which all hydrogens were entered in ideal calculated positions and constrained to riding motion, with a single variable isotropic temperature factor. The C-11 methyl group orientation was determined by analysis of difference electron density maps. After all shift/esd ratios were less than 0·1, convergence was reached at the agreement factors listed above. No unusually high correlations were noted between any of the variables in the last cycle of full-matrix least-squares refinement, and the final difference density map showed a maximum peak of about 0·7 e $Å^{-3}$ located near Re. All calculations were made using the Nicolet SHELXTL PLUS (1987) series of crystallographic programs.

ACKNOWLEDGMENTS

We thank the National Science Foundation, the Robert A. Welch Foundation and the Texas Advanced Research Program for financial support.

REFERENCES

1. F. G. Bordwell, T. A. Cripe and D. L. Hughes in *Nucleophilicity*, edited by J. M. Harris and S. P. McManus, p. 137. American Chemical Society, Washington, DC (1987).
2. (a) F. G. Bordwell and M. J. Bausch, *J. Am. Chem. Soc.* **108**, 1979 (1986); (b) F. G. Bordwell and J. A. Harrelson, Jr, *J. Org. Chem.* **54**, 4893 (1989).
3. (a) C. D. Ritchie, *Can J. Chem.* **64**, 2239 (1986); (b) C. D. Ritchie, *J. Am. Chem. Soc.* **105**, 7313 (1983).
4. R. A. Flowers and E. M. Arnett, *Chem. Soc. Rev.* 9 (1993).
5. (a) S. S. Shaik and A. Pross, *Acc. Chem. Res.* **16**, 363 (1983); (b) S. S. Shaik, *Prog. Phys. Org. Chem.* **15**, 197 (1985); (c) A. Pross and S. S. Shaik, *New J. Chem.* **13**, 427 (1989); (d) S. Shaik, *J. Mol. Liq.* **61**, 49 (1994).
6. (a) S. Hoz, in Ref. 1a, p. 181; (b) K. Fuji in ref. 1, p. 219; (c) I. Lee, *Adv. Phys. Org. Chem.* **27**, 57 (1992).
7. (a) Y. Dakhnovskii, *J. Mol. Liq.* **60**, 73 (1994); (b) A. A. Stuchebrukhov and Y. Y. Song, *J. Chem. Phys.* **101**, 9354 (1994).
8. J. K. Kochi, *Angew. Chem., Int. Ed. Engl.* **27**, 1227 (1988).
9. H. Taube and E. S. Gould, *Acc. Chem. Res.* **2**, 1225 (1969).
10. C. G. C. Waschewsky, P. W. Kash, T. L. Myers, D. C. Kitchen and L. J. Butler, *J. Chem. Soc., Faraday Trans.* **90**, 1581 (1994).
11. J. E. Ellis, *J. Organomet. Chem.* **86**, 1 (1975).
12. (a) S. Henderson and R. A. Henderson, *Adv. Phys. Org. Chem.* **23**, 1 (1987); (b) R. G. Pearson, *Chem. Rev.* **85**, 41 (1985); (c) R. G. Pearson and P. E. Figdore, *J. Am. Chem. Soc.* **102**, 1541 (1980).
13. C.-K. Lai, W. G. Feighery, Y. Zhen and J. D. Atwood, *Inorg. Chem.* **28**, 3929 (1989).
14. (a) R. E. Dessy, F. E. Stary, R. B. King and M. Waldrop, *J. Am. Chem. Soc.* **87**, 453, 460, 467, 471 (1965); (b) N. G. Connelly and W. E. Geiger, *Adv. Organomet. Chem.* **23**, 1 (1984).
15. (a) R. E. Dessy, R. L. Pohl and R. B. King, *J. Am. Chem. Soc.* **88**, 5121 (1966); (b) S. Wolfe, S. Hoz, D. Cohen and M. Liuneh, *Isr. J. Chem.* **29**, 221 (1989).
16. (a) A. J. Pearson and J. Yoon, *Tetrahedron Lett.* **26**, 2399 (1985); (b) A. J. Pearson, S. A. Kole and T. Ray, *J. Am. Chem. Soc.* **106**, 6060 (1984); (c) T. Kruck, M. Hoeffler and M. Noack, *Chem. Ber.* **99**, 1153 (1966).
17. (a) R. E. Lehmann, T. M. Bockman and J. K. Kochi, *J. Am. Chem. Soc.* **112**, 458 (1990); (b) R. E. Lehmann and J. K. Kochi, *Organometallics* **10**, 190 (1991); (c) K. Y. Lee, D. J. Kuchynka and J. K. Kochi, *Organometallics* **6**, 1886 (1987); (d) K. Y. Lee and J. K. Kochi, *Inorg. Chem.* **28**, 567 (1989).
18. (a) J. D. Atwood, *Inorg. Chem.* **26**, 2918 (1987); (b) Y. Q. Zhen, W. G. Feighery and J. D. Atwood, *J. Am. Chem. Soc.* **113**, 3616 (1991); (c) Y. Q. Zhen and J. D. Atwood, *J. Coord. Chem.* **25**, 229 (1992); (d) W. S. Striejewske, R. F. See, M. R. Churchill and J. D. Atwood, *Organometallics* **12**, 4413 (1993).
19. (a) W. Beck and K. Sünkel, *Chem. Rev.* **88**, 1405 (1988); (b) W. Beck, B. Niemer and M. Wieser, *Angew. Chem., Int. Ed. Engl.* **32**, 923 (1993).
20. (a) R. B. King, *Acc. Chem. Res.* **3**, 417 (1970); (b) L. S. Crocker, B. M. Mattson and D. M. Heinekey, *Organometallics* **9**, 1011 (1990); (c) E. K. Barefield and D. J. Sepelak, *J. Am. Chem. Soc.* **101**, 6542 (1979); (d) M. Y. Darensbourg, C. E. Ash, L. W. Arndt, C. P. Janzen, K. A. Youngdahl and Y. K. Park, *J. Organomet. Chem.* **383**, 191 (1990).
21. N. M. Boag and H. D. Kaesz, in *Comprehensive Organometallic Chemistry*, edited by G. Wilkinson, F. G. A. Stone and E. W. Abel, Vol. 4, p. 1161. Pergamon Press, Oxford (1982).
22. V. D. Parker and M. Tilset, *J. Am. Chem. Soc.* **111**, 6711 (1989).
23. (a) R. D. Closson, J. Kozikowski and T. H. Coffield, *J. Org. Chem.* **22**, 598 (1957); (b) R. W. Johnson and R. G. Pearson, *J. Chem. Soc., Chem. Commun.* 986 (1970); (c) C. M. Lukehart, G. P. Torrence and J. V. Zeile, *Inorg. Synth.* **18**, 57 (1978).
24. (a) K. Raab, U. Nagel and W. Beck, *Z. Naturforsch., Teil B* **838**, 1466 (1983); (b) B. Olgemöller and W. Beck, *Chem. Ber.* **114**, 867 (1981); (c) R. C. Bush, R. A. Jacobson and R. J. Angelici, *J. Organomet. Chem.* **323**, C25 (1982).
25. A. R. Katritzky, K. Sakizadeh and G. Musumarra, *Heterocycles* **23**, 1765 (1985).
26. A. R. Katritzky and G. Musumarra, *Chem. Soc. Rev.* **13**, 47 (1984).
27. D. L. Comins and S. O'Connor, *Adv. Heterocycl. Chem.* **44**, 199 (1988).
28. (a) T. M. Bockman and J. K. Kochi, *J. Am. Chem. Soc.* **110**, 1294 (1988); (b) T. M. Bockman and J. K. Kochi, *J. Am. Chem. Soc.* **111**, 4669 (1989).
29. (a) T. M. Bockman and J. K. Kochi, *Adv. Organomet. Chem.* **33**, 52 (1991); (b) T. M. Bockman and J. K. Kochi, *J. Chem. Soc., Perkin Trans 2* 1901 (1994).
30. (a) C.-H. Wei, T. M. Bockman and J. K. Kochi, *J. Organomet. Chem.* **428**, 85 (1992); (b) C.-H. Wei and J. K. Kochi, *J. Organomet. Chem.* **451**, 111 (1993).
31. (a) F. Calderazzo, G. Pampaloni, M. Lanfranchi and G. Pelizzi, *J. Organomet. Chem.* **296**, 1 (1986); (b) F. Calderazzo, G. Pampaloni, G. Pelizzi and F. Vitali, *Organometallics* **7**, 1083 (1988).
32. (a) A. Vogler and H. Kunkely, *Organometallics* **7**, 1440 (1988); (b) A. Vogler and H. Kunkely, *Top. Curr. Chem.* **158**, 24 (1990).

33. Y. Zhen, W. G. Feighery, C.-K. Lai and J. D. Atwood, *J. Am. Chem. Soc.* **111**, 7832 (1989).
34. D. M. Heinekey and W. A. G. Graham, *J. Organomet. Chem.* **232**, 335 (1982).
35. P. S. Braterman, *Metal Carbonyl Spectra*, p. 198. Academic Press, New York (1975).
36. N. S. Kopper, S. A. Jonker, J. W. Verhoeven and C. van Dijk, *Recl. Trav. Chim. Pays-Bas* **104**, 296 (1985).
37. H. Göth, P. Cerutti and H. Schmid, *Helv. Chim. Acta* **48**, 1395 (1965).
38. S. Kato, J. Nakaya and E. Imoto, *Denki Kagaku*, **40**, 708 (1972); *Chem. Abstr.* **78**, 91770.
39. R. S. Mulliken, *J. Am. Chem. Soc.* **74**, 811 (1956).
40. (a) L. J. Rothberg, N. J. Cooper, K. S. Peters and V. Vaides, *J. Am. Chem. Soc.* **104**, 3536 (1982); (b) H. W. Walker, R. S. Herrick, R. J. Olsen and T. L. Brown, *J. Am. Chem. Soc.* **23**, 3748 (1982).
41. (a) R. S. Herrick, *Rev. Inorg. Chem.* **8**, 1 (1986); (b) T. J. Meyer and J. V. Caspar, *Chem. Rev.* **85**, 187 (1985).
42. J. W. Bunting, *Tetrahedron* **43**, 4277 (1987).
43. J. W. Bunting, V. S. F. Chew and S. Sindhautmadja, *Can. J. Chem.* **59**, 3159 (1981).
44. (a) S. Kitane, K. Tshiamala, B. Lande, J. Vebrel and E. Cerutti, *Tetrahedron* **41**, 3737 (1985); (b) S. Oae and N. Furukawa, *Adv. Heterocycl. Chem.* **48**, 1 (1990).
45. J. G. Keay, *Adv. Heterocycl. Chem.* **39**, 1 (1986).
46. (a) G. Illuminati, *Adv. Heterocycl. Chem.* **3**, 285 (1964); (b) I. Takeuchi, Y. Shibata and Y. Hamada, *Heterocycles* **23**, 1635 (1985); (c) V. N. Charushin, O. N. Chupakhin, E. O. Sidorov, J. Beilis and I. A. Terenteva, *Zh. Org. Khim.* **14**, 140 (1978).
47. G. L. Geoffroy and M. S. Wrighton, *Organometallic Photochemistry*, p. 19. Academic Press, New York (1979).
48. (a) C. L. Bird and A. T. Kuhn, *Chem. Soc. Rev.* **10**, 49 (1981); (b) T. M. Bockman and J. K. Kochi, *J. Org. Chem.* **55**, 4127 (1990).
49. M. A. Oturan, P. Dostert, M. Strolin Benedetti, J. Moiroux, A. Anne and M. B. Fleury, *J. Electroanal. Chem.* **242**, 171 (1988).
50. A. Webber, E. Kirowa-Eisner, J. Osteryoung and J. Hermolin, *J. Electrochem. Soc.* **129**, 2727 (1982).
51. (a) B. A. Frenz and J. A. Ibers, *Inorg. Chem.* **11**, 1109 (1972); (b) M. Shauna Corraine, C. K. Lai, Y. Zhen, M. R. Churchill, L. A. Buttrey, JK. W. Ziller and J. D. Atwood, *Organometallics* **11**, 35 (1992); (c) G. Kong, G. N. Harakas and B. R. Whittlesey, *J. Am. Chem. Soc.* **117**, 3502 (1995).
52. J. M. Boncella and R. A. Anderson, *Inorg. Chem.* **23**, 432 (1984).
53. G. Al-Takhin, J. A. Connor and H. A. Skinner, *J. Organomet. Chem.* **259**, 313 (1983).
54. J. A. Connor, M. T. Zafarani-Moattar, J. Bickerton, N. I. El Saied, S. Suradi, R. Carson, G. Al-Taklin and H. A. Skinner, *Organometallics* **1**, 1166 (1982).
55. A. K. Campen, R. Narayanaswamy and A. J. Rest, *J. Chem. Soc., Dalton Trans.* 823 (1990).
56. S. Fukuzumi and J. K. Kochi, *J. Am. Chem. Soc.* **104**, 7599 (1982).
57. (a) H. Huber, E. P. Kundig and G. A. Ozin, *J. Am. Chem. Soc.* **96**, 5585 (1974); (b) S. P. Church, M. Poliakoff, J. A. Timney and J. J. Turner, *J. Am. Chem. Soc.* **103**, 7515 (1981).
58. M. C. R. Symons and R. L. Sweany, *Organometallics* **1**, 834 (1982).
59. (a) R. A. Marcus, *Annu. Rev. Phys. Chem.* **15**, 155 (1964); (b) R. A. Marcus, *J. Chem. Phys.* **24**, 966 (1956).
60. R. A. Marcus, *J. Phys. Chem.* **93**, 3078 (1989).
61. J. K. Ruff and W. J. Schlienz, *Inorg. Synth.* **15**, 87 (1972).
62. G. Maas and B. Singer, *Z. Naturforsch., Teil B* **40**, 90 (1985).
63. A. Katritzky and W. H. Ramer, *J. Org. Chem.* **50**, 852 (1985).
64. R. A. Faltynek and M. S. Wrighton, *J. Am. Chem. Soc.* **100**, 2701 (1978).
65. D. Drew, D. J. Darensbourg and M. Y. Darensbourg, *Inorg. Chem.* **14**, 1579 (1975).
66. A. Anne, P. Hapiot, J. Moiroux, P. Neta and J.-M. Savéant, *J. Am. Chem. Soc.* **114**, 4694 (1992).
67. For diffusion-controlled dimerization, see S. L. Murov, I. Carmichael and G. L. Hug, *Handbook of Photochemistry*, 2nd ed., p. 207. Marcel Dekker, New York (1993).

